LANDSLIDE SUSCEPTIBILITY MAPPING USING GIS BASED PROBABILISTIC APPROACHES IN KALIMPONG AND DARJEELING, WEST BENGAL, INDIA

A DISSERTATION

SUBMITTED IN PARTIAL FULFILLMENT OF THE
REQUIREMENT FOR THE AWARD OF THE DEGREE OF

MASTER OF TECHNOLOGY

IN

GEOTECHNICAL ENGINEERING

Submitted by:

PARTH JAIN

(2K21/GTE/12)

Under the Supervision of

Prof. KONGAN ARYAN

DEPARTMENT OF CIVIL ENGINEERING

DELHI TECHNOLOGICAL UNIVERSITY

(Formerly Delhi College of Engineering)

Bawana Road, Delhi-110042

MAY 2023

DEPARTMENT OF CIVIL ENGINEERING

DELHI TECHNOLOGICAL UNIVERSITY

(Formerly Delhi College of Engineering)

Bawana Road, Delhi-110042

CANDIDATE'S DECLARATION

I, Parth Jain, Roll No. 2K21/GTE/12, a student of M.Tech. in Geotechnical Engineering, declare that the project Dissertation titled "Landslide susceptibility mapping using GIS-based probabilistic approaches in Kalimpong-Darjeeling, West Bengal, India," which is submitted by me to the Department of Civil Engineering, Delhi Technological University, Delhi for the partial fulfillment of the requirement for the award of the degree of Master of Technology, is original and not copied from any source without proper citation. This work has not previously formed the basis for the award of any Degree, Diploma Associateship, Fellowship or other similar title or recognition.

Place: Delhi

PARTH JAIN

Date: .05.2023

DEPARTMENT OF CIVIL ENGINEERING

DELHI TECHNOLOGICAL UNIVERSITY

(Formerly Delhi College of Engineering)

Bawana Road, Delhi-110042

CERTIFICATE

I hereby certify that the Project Dissertation titled "Landslide susceptibility mapping using GIS-based probabilistic approaches in Kalimpong-Darjeeling, West Bengal, India" which is submitted by Parth Jain; Roll No – 2K21/GTE/12; Department of Civil Engineering, Delhi Technological University, Delhi for the partial fulfillment of the requirement for the award of the degree of Master of Technology, is a record of the project work carried out by the student under my supervision. To the best of my knowledge, this work has not been submitted in part or full for any Degree or Diploma to this University or elsewhere.

Place: Delhi

Date: .05.2023

Prof. KONGAN ARYAN

SUPERVISOR

ABSTRACT

In West Bengal, India's Darjeeling Kalimpong area, landslides are a serious concern. With the use of four GIS-based techniques, including the Shannon Entropy (SE), Statistical Index Method (SIM), and Weight-of-Evidence (WoE), this study attempts to create an extensive map of landslip susceptibility. These techniques were chosen because they are good at managing huge datasets, tolerating various factors, and giving reliable estimates of landslip vulnerability. The research area was split into two parts: the first was for training the models, and the second was for model validation. A total of 13 conditioning factors were chosen and examined for their impact on the likelihood of landslides, including elevation, slope, aspect, curvature, distance from rivers, roads, and lineaments, lithology, land use/cover, stream power index, topographic wetness index, rainfall, and geology. Each strategy was put into practise, and the resulting maps of landslip susceptibility were compared and assessed. The analysis's findings demonstrated that all four models were useful for estimating the likelihood of landslides, with the SI, and WoE models performing somewhat better than the SE model. The Receiver Operating Characteristic (ROC) curve was used to evaluate the models' accuracy, and it revealed that the SI, SE, and WoE models had AUC values of 0.826, 0.77, and 0.825, respectively. The landslip inventory data was used to evaluate and validate the landslip susceptibility maps produced by the four models. The comparison revealed that for predicting landslip susceptibility, the SI and WoE models performed better than the SE model. This work provides useful data for land use planning and disaster management in the study region and shows the efficiency of GIS-based models in landslip susceptibility mapping.

ACKNOWLEDGEMENTS

My two-year master's degree in geotechnical engineering from Delhi Technological University (DTU), New Delhi, India, culminated in the research project that follows. In order for this effort to have been effective, I would like to sincerely thank the employees at Delhi Technological University (DTU) for their swift academic and administrative support.

I appreciate Prof. Kongan Aryan, my thesis advisor, for his insightful advice and enlightening criticism while I planned and carried out my research work. Without his prompt contributions and regular evaluations, this project would not have produced the anticipated outcomes.

I would want to express my sincere gratitude to my family for their ongoing support and encouragement in helping me finish the course. Additionally, I want to express my gratitude to my college buddies who I spent the entire academic year studying with and who helped me obtain invaluable experiences that allowed me to try to delve deep into the world of knowledge.

PARTH JAIN

TABLE OF CONTENTS

LIST OF TABLES

LIST OF FIGURES

CHAPTER 1 - INTRODUCTION

1.1 Background and Purpose of Study:

In hilly and mountainous areas around the world, including India, landslides are a frequent natural danger. The Darjeeling Kalimpong district in West Bengal, India's northeast, is distinguished for its varied topography, which includes steep hills and intricate geological formations. Due to these innate qualities, landslides are more likely to occur in the district. Significant landslides have occurred in the area over time, causing fatalities, the damage of infrastructure, and the disruption of socioeconomic activities. The region's vulnerability to landslides is further increased by the steep topography and heavy monsoon rainfall. The area is more susceptible to landslides due to the mountainous topography and heavy rain during the monsoon season. It is essential for efficient land use planning, disaster management, and mitigation activities to have a thorough understanding of the elements influencing landslip susceptibility and an accurate map of the areas at risk.

Due to its capacity to handle enormous datasets, combine several parameters, and produce precise findings, the geographic information system (GIS) has emerged as a crucial instrument in the mapping of landslip susceptibility. The Statistical Index Method (SIM), Shannon Entropy (SE), and Weight-of-Evidence (WoE) methodologies have all been utilised for landslip susceptibility mapping. Due to their capacity to handle big datasets, combine various variables, and produce precise findings, these methodologies have been frequently used. However, depending on the study region and the variables influencing landslip occurrence, its efficacy differs.

The necessity to thoroughly evaluate and reduce the dangers connected with landslides in the Darjeeling Kalimpong district is the driving force for this study. The complicated interactions between different contributing components are frequently difficult to capture using traditional landslip susceptibility mapping techniques. In order to improve the precision and dependability of landslip susceptibility evaluations, there is a growing interest in utilising cutting-edge Geographic Information System (GIS)-based approaches. This work intends to

generate detailed landslip susceptibility maps tailored to the study area using the Shannon Entropy, Statistical Index Method, and Weight-of-Evidence techniques. The study aims to offer useful insights into the spatial distribution and extent of landslide-prone areas by integrating different conditioning factors and using cutting-edge modelling approaches.

The Darjeeling-Kalimpong region of India as well as other areas with a comparable geography can benefit greatly from the study's findings for both land use planning and disaster management. The models' landslide susceptibility maps will be helpful for locating regions with a high risk of landslides and for determining the best course of action to reduce the risks. The study will also shed light on the variables that affect landslip occurrence in the Darjeeling-Kalimpong region and offer suggestions for future research in this field.

1.2 Aim of the Study:

The objectives of this study are to create a map of landslip susceptibility for the West Bengal, India, districts of Darjeeling and Kalimpong using four different GIS-based approaches (FR, SIM, SE, and WoE), to assess the utility of each approach, and to confirm the precision of the models using the ROC curve. This study also seeks to provide insights into the conditions that contribute to landslip susceptibility, analyse the impact of different influencing factors on landslip occurrence in the study area, and provide a helpful tool for disaster management and land-use planning in the area. Finally, this study intends to add to the body of knowledge on landslip susceptibility mapping in mountainous areas with complex geology and high rainfall, as well as to evaluate the methodologies utilised, point out their advantages and disadvantages, and make suggestions for further study.

For the parties involved in landslip risk management and sustainable development in the Darjeeling Kalimpong district, this research has important academic and practical ramifications. The study aims to improve the accuracy and reliability of landslip susceptibility mapping through the use of cutting-edge GIS-based techniques, enabling more efficient decision-making. The results of this study can help land managers and urban planners identify high-risk regions, put effective land use zoning policies into practise, and create focused mitigation measures to lessen the effects of landslides.

1.3 Objectives:

The main research objectives formulated for this research work have been outlined as:

- To determine and evaluate the environmental conditions influencing the district of Darjeeling and Kalimpong's susceptibility to landslides: Slope, aspect, elevation, geology, land use/cover, rainfall patterns, and proximity to roads and rivers are just a few of the variables that must be thoroughly reviewed and analysed in this regard. Building accurate and trustworthy landslip susceptibility models requires a thorough understanding of these components and how they affect landslip occurrences.

- To create maps of landslip susceptibility using GIS-based methods: To create spatially detailed landslip susceptibility maps, the study will use the Shannon Entropy, Statistical Index Method, and Weight-of-Evidence techniques. These cutting-edge approaches enable the attribution of susceptibility values to various regions within the research region and facilitate the integration of numerous variables.

- To compare and assess the merits of the various methods for determining landslip susceptibility in the research area: To evaluate each method's effectiveness and determine its advantages and disadvantages in identifying landslip susceptibility patterns, a comparison study of the results from the various ways will be done. This assessment will help determine the best method, or methods in combination, for mapping the susceptibility to landslides in the Darjeeling Kalimpong district.

- To offer suggestions for land use planning and disaster management: Based on the study's findings, useful suggestions will be crafted to help land managers, urban planners, and policymakers decide on the best course of action for infrastructure development, disaster risk reduction, and land use zoning. These suggestions are meant to lessen landslip vulnerability in communities and encourage sustainable development methods in the research region.

CHAPTER 2 - LITERATURE REVIEW

2.1 Definition and Mechanism of Landslides:

A mass of rock, soil, or debris sliding down a slope or a steep incline is referred to as a landslip. It is a type of natural geohazard that develops as a result of a confluence of environmental, geomorphological, and geological causes. Heavy rainfall, seismic activity, slope instability, and human activities like deforestation or incorrect land use are just a few of the factors that can produce landslides. A landslide's material movement can range from gradual creeping to swift and devastating sliding, posing serious dangers to infrastructure, the environment, and human life. Landslides have the potential to change the natural landscape, cause property damage, impede transportation, and take lives. In order to assess landslide susceptibility, create efficient mitigation methods, and put land use planning plans into action to lessen the effects of this dangerous event, it is essential to understand the causes and mechanisms of landslides.

The complex combination of geological, geomorphological, and environmental elements that causes landslides. For estimating their frequency and putting appropriate mitigation measures in place, it is essential to understand the mechanisms underlying landslides. Depending on the type of landslide—falls, slides, flows, and complex combinations of these movements—the mechanism can change.

Falls: Falls happen when objects like rocks or debris fall through the air after breaking free from a cliff or other steep slope. These weathering processes, such as erosion, freeze-thaw cycles, or the undercutting of the slope's base by rivers or waves, frequently cause these landslides.

Slides: In slides, materials are moved along clearly defined surfaces called shear planes. The rotational slide, in which the materials move down a concave curved surface, is the most typical kind of slide. This kind of landslip frequently happens in solid rock formations or cohesive soils. While translational slides include the movement of materials along a flat surface, they often take place in bedrock with obvious bedding planes or joints or in non-

cohesive soils.

Flows: When a mass of viscous or turbulent material slides down a slope, it is referred to as a flow. Depending on the make-up and consistency of the material involved, these movements can also be divided into debris flows, mudflows, and avalanches. While mudflows primarily involve water and fine-grained sediments, debris flows also contain water, soil, and rock pieces.

Slope gradient, geology, soil characteristics, groundwater conditions, and external triggers like rainfall or seismic activity are among the variables influencing landslip mechanisms. These elements may weaken the materials that make up the slope, lessen their internal strength, or raise pore water pressure, which would enhance their susceptibility to failure and movement.

2.2 Software and Tools Incorporated:

For the study, visualisation, and management of geospatial data, remote sensing data are combined with a Geographic Information System (GIS), a potent software tool. ArcGIS is one of the most extensively used GIS programmes, and in particular, version 10.8 provides a complete range of tools and functions for remote sensing applications.

A user-friendly interface for handling and processing remote sensing data is offered by ArcGIS 10.8. It allows for the integration and import of a wide range of remote sensing datasets, including radar imaging, aerial photos, LiDAR data, and satellite photography. By accurately aligning remote sensing data with spatial reference systems thanks to ArcGIS' georeferencing capabilities, precise spatial analysis and interpretation are made possible.

ArcGIS 10.8 has a wide range of uses in remote sensing across many industries. Through image processing methods including picture enhancement, classification, and feature extraction, it makes it easier to retrieve useful information from remote sensing data. Users can do complex analyses using ArcGIS's geospatial analysis features, such as change detection, land cover mapping, and vegetation index calculation.

In order to facilitate thorough geographical analysis, ArcGIS also supports the integration of remote sensing data with other geospatial information. It offers capabilities for proximity analysis, topography analysis, and spatial interpolation, all of which are crucial for environmental monitoring, resource management, and urban planning. ArcGIS also makes it possible to visualise the outcomes of remote sensing through interactive maps, themed layers, and 3D representations, which improves data sharing and decision-making.

ArcGIS 10.8 provides specialised tools and workflows for landslip susceptibility mapping. To create precise susceptibility maps, it enables the integration of several geographic layers, including slope, geology, land cover, and rainfall data. The geoprocessing capabilities in ArcGIS can be used by users to analyse and visualise landslide-prone areas using a variety of methodologies, such as Shannon entropy, statistical index method, and weight-of-evidence.

ArcGIS 10.8 is an all-around capable and flexible GIS programme for remote sensing applications. It is a useful tool for analysing and understanding remote sensing data, allowing informed decision-making, and supporting a wide range of geospatial studies across multiple disciplines because of its comprehensive functions and integration possibilities.

2.3 Review of Studies:

A.Chawla et al. in order to generate a zonation map for landslip susceptibility, conducted research in the Darjeeling District in the Eastern Himalayas of India. Using remote sensing and GIS methods, they investigated a number of landslide-causing factors, including geology, slope, land use, and rainfall. The frequency ratio model was used to corroborate the study's conclusions using information from the landslip inventory. Through the provision of perceptive knowledge about landslide-prone areas, the research aids in the improvement of land management practises and disaster prevention strategies [1].

A.Saha et al., to map the landslip susceptibility in the Darjeeling Himalayas, used artificial neural networks (ANN), fuzzy analytic hierarchy process (AHP), and multicriteria decision analysis (MCDA). The study integrated a variety of factors, including slope, aspect, curvature, geology, land use, and precipitation, to construct a GIS-based landslip susceptibility model. The results demonstrate the effectiveness of the recommended method and the potential applications for guiding risk evaluation and local land use planning [2].

A. Sharma et al. introduced an entropy-based hybrid random forest and support vector machine integration for the assessment of landslip susceptibility. The goal of the study was to improve the accuracy of mapping landslip susceptibility by combining the benefits of the two machine learning approaches. The research used a range of conditioning factors to build the model, including slope, aspect, curvature, lithology, and land cover. The results show how well the hybrid approach evaluates landslip vulnerability and its potential for practical applications [3].

A. Yalcin mapped the landslip susceptibility in Ardesen, Turkey, using bivariate statistics and the analytical hierarchy process (AHP). The study corroborated the results of both techniques by contrasting their outputs using data from landslip inventories. The study provided critical information for regional land use planning and landslip risk management by demonstrating how the AHP and bivariate statistics may be utilised to evaluate landslip susceptibility [4].

A. Yalcin et al. carried out a comparison study of several landslip susceptibility mapping methodologies in Trabzon, NE Turkey. The study using GIS techniques looked at bivariate statistics, the analytical hierarchy process (AHP), the frequency ratio, and logistic regression models. As a result of the findings, which showed that each model performed differently, picking an appropriate strategy based on the distinctive characteristics of the research location is essential for an effective assessment of landslip susceptibility [5].

B. Pradhan and S. Lee investigated the effectiveness of backpropagation artificial neural networks (BP-ANN), frequency ratio (FR), and bivariate logistic regression (BLR) models for determining landslip risk. A number of variables, such as slope, aspect, curvature, lithology, and land cover, were used to build the models. The research demonstrated that when it came to mapping landslip susceptibility, BP-ANN was more effective than FR and BLR models. The findings support improved methods for assessing and mitigating landslip hazards [6].

B. Pradhan et al., in a remote sensing and GIS-based landslip susceptibility investigation, applied the frequency ratio model in three test locations. A multitude of conditioning factors, including slope, aspect, curvature, lithology, land cover, and isolation from roads, were combined to construct the susceptibility map. The study demonstrated the frequency ratio model's usefulness for assessing landslip hazards and planning land uses in the study regions

and used landslip inventory data to support the conclusions [7].

B. T Pham et al., compared Bayesian and Support Vector Machine (SVM) approaches for predicting landslip vulnerability. A number of conditioning factors, such as slope, aspect, curvature, lithology, land cover, and rainfall, were used to create the models. The study focused on the advantages and disadvantages of SVM and Bayesian algorithms for determining landslip susceptibility in challenging terrain and assessed the precision of both models using information from landslip inventory [8].

C. Audisio et al., developed a GIS programme for data entry and risk management of historical instability processes in Italian Alpine river basins. The study focused on applying GIS techniques to investigate and manage landslip concerns by integrating historical data, hazard zonation, and susceptibility mapping. The study demonstrated how the GIS tool is effective in providing pertinent data for determining the danger of landslides and improving risk management and decision-making [9].

C. Van Westen et al., conducted research on the application of GIS techniques for landslip vulnerability mapping. The study stressed the necessity for accurate susceptibility maps that include slope, lithology, land cover, rainfall, and land use, among other conditioning factors. The study clarified the advantages and disadvantages of various modelling methodologies and stressed the need for precise validation procedures for assessing landslip vulnerability [10].

C.-J. F. et al., conducted research on the reliability of spatial prediction models for mapping landslip hazards. Fabbri. The primary goal of the study was to assess the accuracy of several landslip susceptibility models using statistical validation techniques. The study stressed the value of reliable validation methods for evaluating the effectiveness of susceptibility models in practical contexts. By highlighting the advantages and disadvantages of spatial prediction models, the results contribute to improving strategies for assessing and mitigating landslip hazards [11].

D. Pathak developed a knowledge-based technique for mapping landslip hazard in the Himalayas. Using specialised expertise and a geographic information system (GIS), the research combined many landslide-causing factors, such as slope, lithology, land cover, and rainfall. The study demonstrated how well a knowledge-based approach may be used to

identify areas that are prone to landslides. The findings contribute to our understanding of landslip dynamics in the Himalayan region and support the creation of accurate methods for measuring landslip susceptibility [12].

D. T. Khuc et al., for the purpose of determining landslip susceptibility, compared the analytical hierarchy process (AHP) and frequency ratio (FR) techniques. A number of conditioning factors, including as slope, lithology, land cover, and proximity to roads, were used to build the models. The study evaluated the efficacy of both strategies and highlighted the advantages and disadvantages of AHP and FR in assessing landslip susceptibility. The findings provide helpful direction for selecting appropriate methods in landslip hazard assessment [13].

F. Guzzetti et al. underlined the significance of landslip inventory maps as practical tools for addressing landslip concerns. The study underlined the need for systematic data collection and recording on landslips in order to develop accurate inventory maps. The study placed a strong emphasis on using inventory maps to identify the features, frequency, and geographic distribution of landslides. The study contributes to the processes of risk management, hazard assessment, and decision-making while advancing our understanding of landslip dynamics [14].

G. Das and K. Lepcha conducted studies on mapping the susceptibility to landslides in the Relli Khola river basin of the Darjeeling Himalaya, India. The research evaluated the performance of logistic regression (LR) and frequency ratio (FR) models to identify landslide-prone sites. A number of conditioning factors, including as slope, lithology, land cover, and isolation from drainage, were used to build the models. The findings demonstrated how effectively LR and FR models worked in mapping landslip susceptibility and provided crucial information for land use planning and catastrophic risk reduction in the research region [15].

G. Zhang et al. evaluated landslip risk in Huizhou, China, using the statistical index method and the analytic hierarchy process (AHP) technique. A number of conditioning factors, such as slope, lithology, land cover, rainfall, and proximity to roadways, were used to build the models. The study demonstrated the need of a comprehensive approach for identifying landslide-prone areas and clarified the advantages of combining statistical index methods with AHP for mapping landslide susceptibility. The findings aid in the region's improved analysis

of landslip risks and development of mitigating measures [16].

H. Pourghasemi et al. investigated the forecasting capability of the Dempster-Shafer (DS) and weights-of-evidence (WoE) models for mapping landslip vulnerability using GIS techniques. A number of conditioning factors, such as slope, lithology, land cover, rainfall, and proximity to roadways, were used to build the models. The study evaluated both models' efficacy and highlighted the advantages and disadvantages of DS and WoE in determining landslip susceptibility. The findings provide helpful guidance for selecting the appropriate modelling techniques for accurate mapping of landslip threats [17].

H. R. Pourghasemi et al., in a study on mapping the vulnerability of landslides by M, the analytical hierarchy process (AHP), statistical index models, and binary logistic regression were utilised. Aghda Fatemi. The research used a number of conditioning factors, including slope, lithology, land cover, rainfall, and separation from faults, in order to construct the models. The efficiency of each model was examined, as well as its ability to identify areas vulnerable to landslides. The outcomes allow for effective risk management and land use planning strategies, as well as improved mapping approaches for landslip susceptibility [18].

H. R. Pourghasemi et al., used conditional probability models and the index of entropy to map the mapping of landslip susceptibility in the Safarood Basin, Iran. A number of conditioning factors, such as slope, lithology, land cover, rainfall, and proximity to roadways, were used to build the models. The study established the use of conditional probability models and the measure of entropy for identifying landslide-prone areas. The findings aid in the improvement of landslip hazard assessment in the research region and the development of well-informed decisions for disaster management [19].

I. Das et al. investigated the mapping of landslip susceptibility along road corridors in the Indian Himalayas using Bayesian logistic regression models. The research used a number of conditioning factors, including slope, lithology, land cover, rainfall, and proximity to roadways, in order to develop the models. The study emphasised the need of considering road corridors as potential landslide-prone areas and demonstrated the efficacy of Bayesian logistic regression models in predicting landslide threats. The findings provide recommendations for improving the planning for road infrastructure and catastrophic risk management in the Himalayan area [20].

J. Roy and S. Saha conducted research on mapping the susceptibility to landslides in the Darjeeling District in West Bengal, India, using knowledge-driven statistical models. The research considered a number of conditioning factors, including slope, lithology, land cover, and rainfall in order to develop the models. The study not only demonstrated the need of utilising local expertise, but it also demonstrated how effective statistical models are at identifying landslide-prone areas. The findings support informed decision-making for lowering catastrophe risk and better understanding of landslip dynamics in the study area [21].

J. Roy et al. created a special ensemble approach for landslip susceptibility mapping (LSM) in the West Bengal, India, districts of Darjeeling and Kalimpong. By integrating several statistical techniques, including logistic regression, frequency ratio, and weights-of-evidence, the research created an ensemble model. The study demonstrated the advantages of employing an ensemble method to accurately capture the complex spatial patterns related to landslip susceptibility. The findings enable the development of more reliable landslip susceptibility mapping techniques and provide insightful information for effective landslip risk management in the area [22].

L. Ayalew and H. Yamagishi, conducted a research on landslip susceptibility mapping in the Kakuda-Yahiko Mountains in Central Japan using GIS-based logistic regression models. The research's many conditioning factors, such as slope, lithology, land cover, and remoteness from drainage, were used to build the models. The research revealed the spatial relationships between the conditioning factors and landslides and demonstrated how effective the logistic regression models were in identifying landslide-prone areas. The findings aid in the analysis of landslip risks in mountainous locations and the development of mitigation strategies [23].

M. Mohammad et al. examined the utility of the frequency ratio, Dempster-Shafer, and weights-of-evidence models for mapping landslip susceptibility in Golestan Province, Iran. A number of conditioning elements, such as slope, lithology, land cover, rainfall, and closeness to faults, were used to build the models. The study evaluated the capability of each model and listed its advantages and disadvantages for estimating landslip susceptibility. The findings support the selection of appropriate modelling techniques for accurate landslip hazard mapping as well as the informed decision-making for land use planning and disaster management [24].

Nohani et al. used a number of bivariate GIS-based models to investigate the mapping of landslip susceptibility. The research evaluated the efficacy of the logistic regression, frequency ratio, weights-of-evidence, and information value techniques for identifying landslide-prone sites. The study included a number of conditioning factors, including slope, lithology, land cover, and proximity to roadways, in order to develop the models. The findings provided insight into the effectiveness of bivariate models in determining landslip susceptibility as well as the impact that different conditioning factors play in landslip occurrence. The work enhances methods for mapping landslip dangers and encourages effective landslip risk management practises [25].

R. Pellicani et al. developed GIS-based prediction models for regional-scale landslip susceptibility evaluation and risk mapping along transportation routes. The research used a number of conditioning factors, including slope, lithology, land cover, rainfall, and proximity to roadways, in order to develop the models. The study stressed the need of considering road corridors as key regions for evaluating landslip susceptibility and shown how effective predictive models are at locating high-risk areas. The results have significant implications for landslip risk mitigation strategies and planning for road infrastructure [26].

S. Chakraborty and S. Mukhopadhyay conducted study on assessing flood risk in the Coochbehar District of West Bengal, India, utilising the analytical hierarchy process (AHP) and geographic information system (GIS). Despite not having anything to do with landslides, the research employed AHP and GIS to evaluate the likelihood of floods based on slope, land cover, rainfall, and drainage. The study provided data for local flood hazard management and demonstrated the effectiveness of the AHP-GIS method for estimating flood risk [27].

S. Lee and K. Min conducted a statistical investigation of landslip susceptibility in Yongin, Korea. The study employed statistical techniques to assess landslip susceptibility based on a variety of conditioning factors, including slope, lithology, land cover, and rainfall. The study clarified the significance of each conditioning factor and how they impact landslip propensity. The findings improve knowledge of landslip susceptibility in the research region and aid in effective methods for assessing and managing landslip risk [28].

S. Mondal and S. Mandal conducted research on the mapping of landslip susceptibility in the

Darjeeling Himalaya in India using the index of entropy (IOE) model. The study used a variety of conditioning factors, including slope, lithology, land cover, and proximity to roadways, to develop the susceptibility map. The study demonstrated the effectiveness of the IOE model in identifying landslide-prone sites and gave information on the geographical distribution of landslide susceptibility in the region. The findings aid the Darjeeling Himalaya in improving their analysis of landslip risks and the creation of mitigating measures [29].

S. Sarkar et al. calculated landslip susceptibility using the Information Value Method in sections of the Darjeeling Himalayas. Slope, lithology, land cover, rainfall, and distance from faults are a few of the conditioning factors that were integrated into the susceptibility model. The study clarified the relationships between conditioning factors and landslides and provided evidence of the effectiveness of the Information Value Method in identifying landslide-prone areas. The findings support improved landslip hazard assessment as well as more precise decision-making for disaster risk reduction and land use planning in the region [30].

T. L. Saaty et al., the Analytic Hierarchy Process (AHP) was examined along with criticisms of it. Despite having no obvious relation to landslip susceptibility mapping, the research provides insights into the AHP technique and its ability to incorporate subjective evaluations in decision-making. The study highlights the need of transparency and in-depth research while outlining the benefits of using the AHP for difficult decisions [31].

CHAPTER 3 - STUDY AREA

The Darjeeling Kalimpong district in West Bengal, India, is the subject of this thesis's study. The district is situated in the southern foothills of the Eastern Himalayas and is found in the eastern region of the Indian state. Its varied geography, which ranges from steep slopes to rolling hills, defines it.

The district of Darjeeling Kalimpong has a subtropical climate with distinct rainy and dry seasons. The area experiences significant annual rainfall, especially from June to September when it monsoons. The region is quite vulnerable to landslides due to the complicated geology, rough topography, and abundant precipitation.

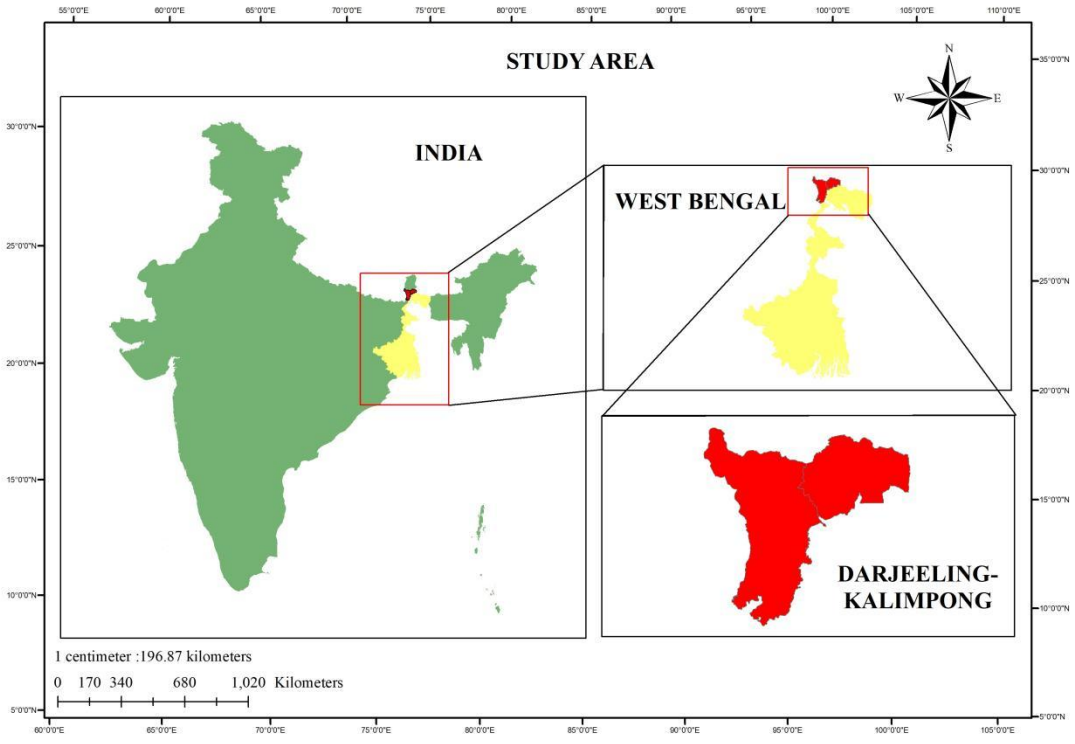

Fig. 3.1 Study Area Map

The study area is well-known for its stunning natural surroundings and ecological importance. It supports many endemic species and provides a vital home for a variety of flora and wildlife, making it rich in biodiversity. Being the home to numerous ethnic populations, including the

native Lepcha, Bhutia, and Nepali communities, the district is also of enormous cultural significance.

This study's primary objective is to map the susceptibility to landslides utilising GIS-based techniques, such as the Shannon Entropy, Statistical Index Method, and Weight-of-Evidence. The goal is to identify landslide-prone areas and provide useful insights for disaster risk management, land use planning, and infrastructure development in the area by integrating various geospatial datasets, including topographic data, geological maps, land cover data, and rainfall patterns.

Overall, because of its distinctive geological setting, difficult topography, and substantial vulnerability to landslides, the Darjeeling Kalimpong district is an ideal study place to examine landslide susceptibility. The findings of this study will advance knowledge of local landslip dynamics and help formulate successful methods for catastrophe risk reduction and sustainable development.

CHAPTER 4 - METHODOLOGY

4.1 Methodology Adopted:

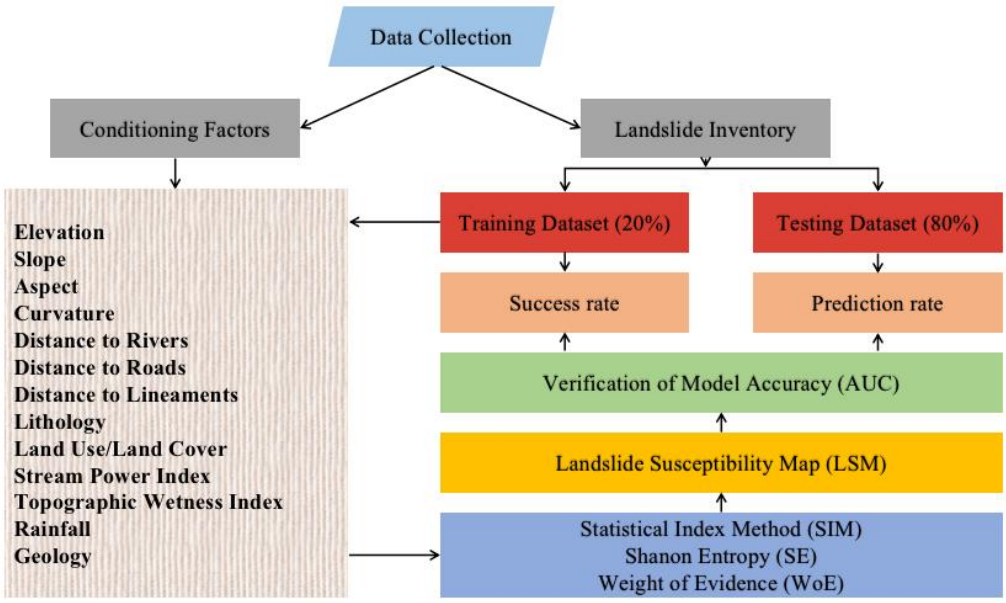

Figure 4.1 Flow Chart of the methods involved

4.1.1 Data Collection

The methodology used in this work uses a thorough method for mapping landslip susceptibility that is based on GIS. The subsequent actions were taken:

4.1.1.1 Acquisition of Remote Sensing Data:

Reliable sources were used to acquire high-resolution satellite imagery, including multispectral and panchromatic data, that covered the study area. In order to extract topographic attributes, digital elevation models (DEMs) with the appropriate spatial resolution were also acquired.

4.1.2 Data Preparation:

4.1.2.1 Image Processing:

To improve the data's quality and clarity, the collected satellite images underwent preprocessing. If numerous scenes were used, this required image mosaicking, radiometric and geometric corrections, atmospheric correction, and so on. Preprocessing was done to maintain uniformity across the dataset, lessen noise, and enhance visual understanding.

4.1.2.2 DEM Processing:

The topographic characteristics slope, aspect, curvature, and topographic wetness index (TWI) were all derived from the DEMs through processing. These factors offer essential details on the features of the terrain and affect the likelihood of landslides.

4.1.3 Landslide Susceptibility Modeling:

4.1.3.1 Selection of Conditioning parameters:

A collection of conditioning parameters impacting landslip susceptibility was determined based on a literature review and expert knowledge. There are a total of 13 conditioning elements, including geology, lithology, land use/cover, slope, aspect, curvature, distance to rivers, distance to roads, distance to lineaments, and stream power index. Every factor was prepared in GIS as a raster layer.

4.1.3.2 Weighting and Integration of Factors:

Depending on their relative significance in the occurrence of landslides, various weighting systems, including Shannon Entropy, Statistical Index Method, and Weight-of-Evidence, were used to assign weights to each conditioning component. A composite landslip susceptibility map was created by combining these weighted components using GIS overlay procedures.

4.1.3.3 Evaluation of Validation and Accuracy:

The Area Under the Receiver Operating Characteristic (ROC) curve was used to assess the accuracy of the landslip susceptibility model. The ROC curve calculates an AUC value by comparing the model's predictions to actual landslides. AUC is a measure of how well a model performs. In order to evaluate the model's capability to detect landslide-prone and non-prone locations, respectively, sensitivity and specificity were also evaluated. These metrics allowed for a thorough assessment of the model's precision and dependability.

4.1.4 Tools and Software:

The main software for processing, analysing, and visualising data was ArcGIS 10.8. The ArcGIS Spatial Analyst and Geostatistical Analyst extensions were used to carry out the various geospatial operations, such as raster calculations, overlay analysis, and statistical modelling.

In order to evaluate landslip susceptibility in the research area, the methodology used in this

work includes remote sensing data processing, GIS tools, and statistical modelling. A thorough understanding of the spatial distribution and potential causes of landslides is made possible by the integration of different conditioning elements. For the Darjeeling Kalimpong district's land use planning, infrastructure development, and catastrophe risk reduction initiatives, the accuracy evaluation verifies the dependability of the created landslip susceptibility map.

4.2 Data used:

4.2.1 Remote Sensing Data:

For this investigation, high-resolution satellite images of the Darjeeling Kalimpong district were acquired. Reliable sources provided the multispectral and panchromatic data for the satellite imagery. In order to reduce the impact of cloud cover and atmospheric conditions on image quality, imagery was gathered during the dry season.

4.2.2 Digital Elevation Models (DEMs):

To extract topographic data, Digital Elevation Models with the appropriate spatial resolution were obtained. The DEMs were gathered from trustworthy sources and accurately depicted the research area's terrain elevation.

4.2.3 Conditioning Factors:

The landslip susceptibility analysis took into account the following 13 conditioning factors:

Elevation: The DEM-derived elevation data revealed details about the terrain's vertical variance.

Slope: To gauge how steep the landscape was, a high-resolution slope map created from the DEMs was employed.

Aspect: Data from the DEMs' aspects gave us insights regarding the slope's orientation's

direction. Convex and concave landforms could be identified by the examination of curvature using DEMs.

Distance to Rivers: To assess how close certain locations are to probable water flow routes, geospatial data depicting rivers and watercourses were employed.

Distance to Roads: Road network data that were collected from trustworthy sources allowed for the assessment of an area's distance from roadways, which can be used as a sign of nearby habitation and probable slope disruptions.

Distance to Lineaments: Lineament data were used to analyse the distance between areas and linear features, which can reveal structural flaws and perhaps landslide-prone terrain.

Lithology: The various rock types found in the research area were identified using geologic maps.

Land Use/Land Cover: The study area was divided into various land cover classes, such as woods, agricultural land, and urban areas, using land cover data derived from satellite imagery or already-existing land cover maps.

Stream Power Index: The SPI, which was produced from DEMs, provides details on the stream erosional power, which has an impact on slope stability.

Topographic Wetness Index: Areas with increased soil moisture content and potential for water accumulation were identified by the topographic wetness index, which was calculated from the DEMs.

Rainfall: To analyse rainfall patterns and pinpoint regions with high precipitation, historical rainfall data from meteorological stations within the study area were employed.

Geology: To identify the various geological formations and evaluate their impact on landslip occurrence, detailed geological maps were used.

The information required for the analysis and modelling of landslip susceptibility in the

Darjeeling Kalimpong district was provided by the data used in this work, which included remote sensing imagery, DEMs, and the thirteen conditioning elements.

Table 4.1 Data and Sources

DATA USED	DATA SOURCES
Digital Elevation Model	Open Topography SRTM GLI Global
Lithology, Geology, Roads, Rivers, Lineaments, Landslide Points	Bhukosh Portal, Geological Survey of India
Rainfall	Climate Research Unit
LULC	ESRI
Indian District Shapefile	Advances in Geographical Research

The Digital Elevation Model (DEM) was created using SRTM GL1 data with a spatial resolution of 30m that was made accessible on an open-source Open Topography portal. Maps of several parameters, including slope, aspect, curvature, and elevation, were produced using the derived DEM. As they have an impact on landslip incidence either directly or indirectly, these elements can be used as landslip causative factors. These elements will also be taken into consideration while creating themed maps, which will be displayed in the following sections. The World Geodetic System 1984 in Universal Transverse Mercator zone 45N was used as the DEM's projected coordinate system instead of the geographic coordinate system since mapping for the DEM was required.

4.3 Derivatives Obtained from DEM:

In this research investigation, DEM data on slope, aspect, curvature, TWI, and SPI were gathered. They were all brought out for the Darjeeling-Kalimpung research area.

4.3.1 Slope:

Slope is a measurement of the terrain's steepness that is generated from the Digital Elevation Model (DEM). It is a crucial component of landslide susceptibility mapping, giving information on regions vulnerable to landslides based on the slope inclination. In order to analyse and reduce the risk of landslides, slope analysis is crucial. Steeper slopes indicate a higher landslide susceptibility. The "Spatial Analyst" tool in ArcGIS was used to extract the slope map from the DEM. In figure 4.2, a detailed slope map is displayed.

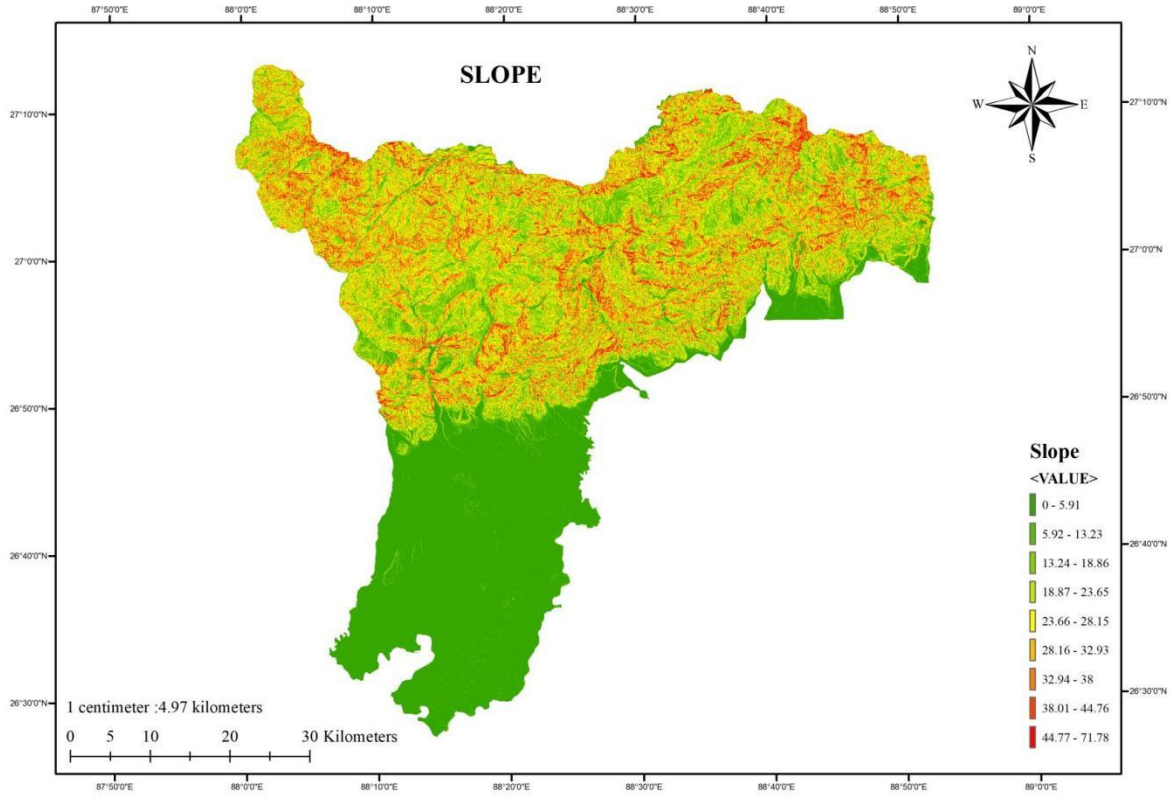

Fig. 4.2 Slope map

4.3.2 Aspect:

A slope's aspect, which is obtained from the Digital Elevation Model (DEM), shows which way it faces. The software interprets the lack of an aspect for flat surfaces as (-1) and indicates this with grey cells in the aspect map. It is an important factor to consider when analysing the characteristics of the terrain, including solar radiation exposure, hydrological patterns, and potential influences on the occurrence of landslides. In figure 4.3, the detailed aspect map is displayed.

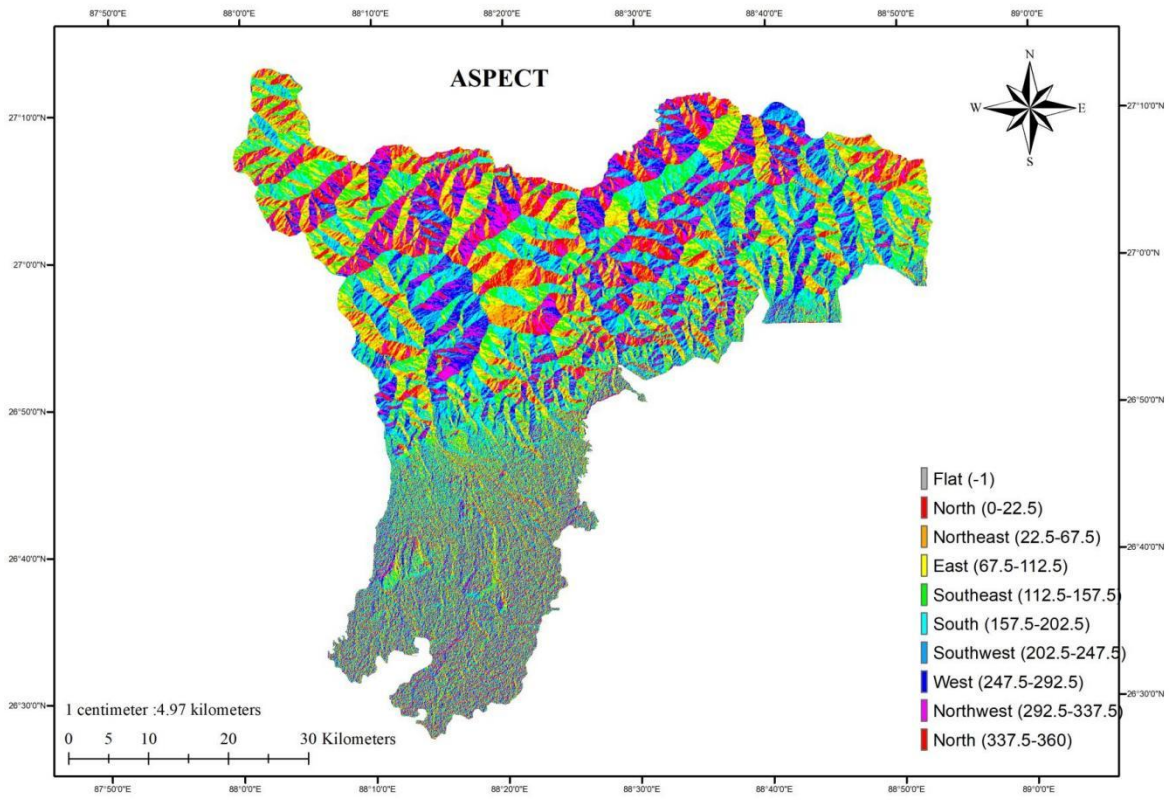

Fig. 4.3 Aspect map

4.3.3 Curvature:

The rate of change in slope along the surface of the terrain is measured by curvature, which is generated from the Digital Elevation Model (DEM). It reveals details about the form and contour of the landscape. Convex or concave curvature can be used to describe whether the landscape is bending outward or inward, respectively.

In order to pinpoint possible instability, curves are crucial in landslip susceptibility mapping. Due to the concentration of gravitational forces, convex landforms with positive curvature are more vulnerable to landslides, whereas concave landforms with negative curvature may suggest areas of material accumulation and improved stability.

Curvature analysis can help identify high-risk sites and guide the development of effective mitigation strategies by revealing locations with specific topographical features and evaluating their impact on landslip occurrence. Figure 4.4 illustrates the comprehensive curvature map.

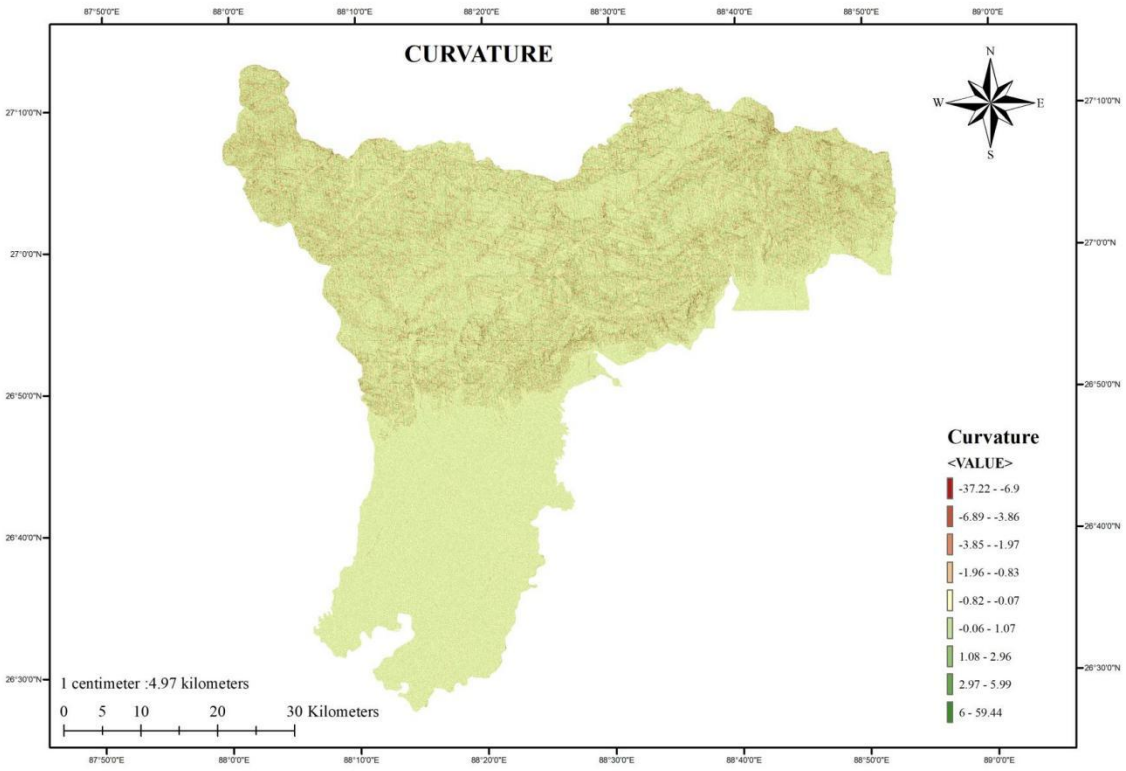

Fig. 4.4 Curvature map

4.3.4 Elevation:

Elevation is the vertical height of the ground above a reference level as determined by the Digital Elevation Model (DEM). It is a key component of geospatial analysis, which includes mapping landslip risk. Elevation offers information about the topographic features of the landscape, making it possible to identify regions with higher elevations that may have increased landslip susceptibility because of things like gravitational forces, slope instability, or the presence of particular geological formations.

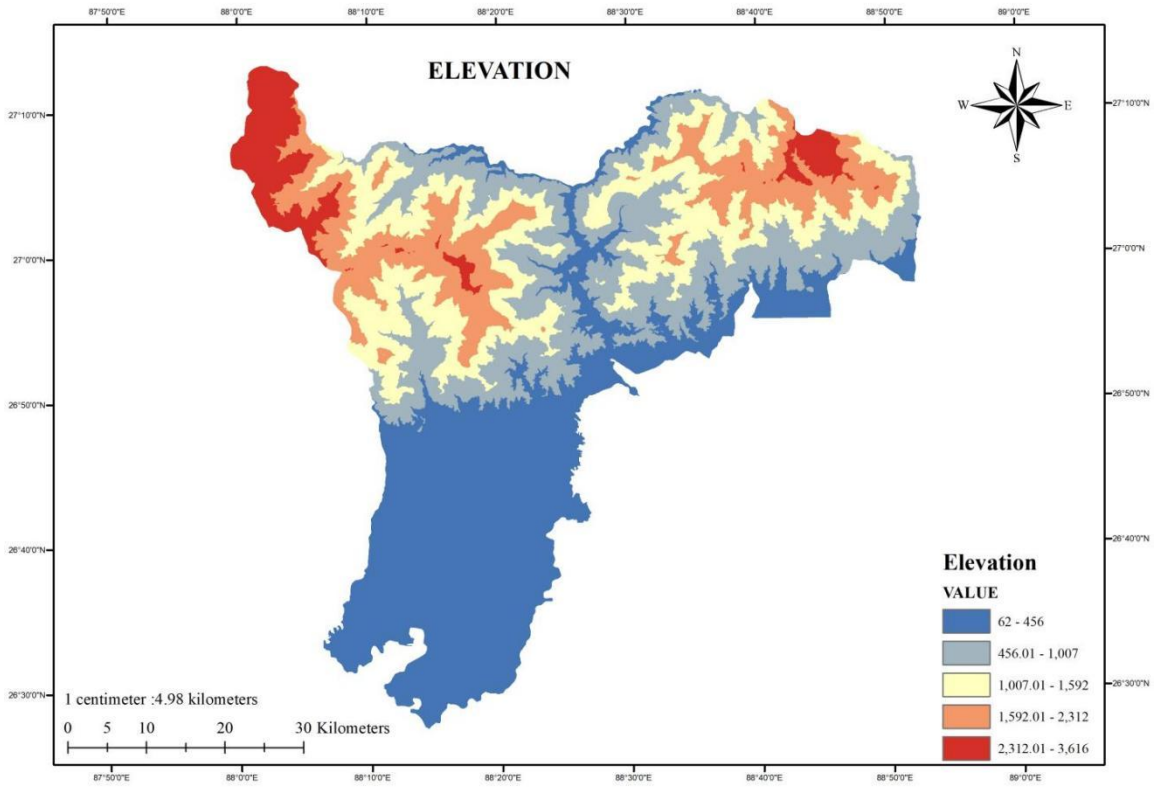

Fig. 4.5 Elevation map

4.3.5 Topographic Wetness Index:

The potential for wetness or water accumulation in the terrain is measured by the Topographic Wetness Index (TWI), which is produced from the Digital Elevation Model (DEM). It takes into account how slope and upslope contributing area are related, offering details on regions susceptible to water saturation and elevated soil moisture, which can affect landslip susceptibility.

TWI is determined numerically as follows:

TWI= Ln (Flow Accumulation+0.001)/ (Slope in Percentage/100+0.001)

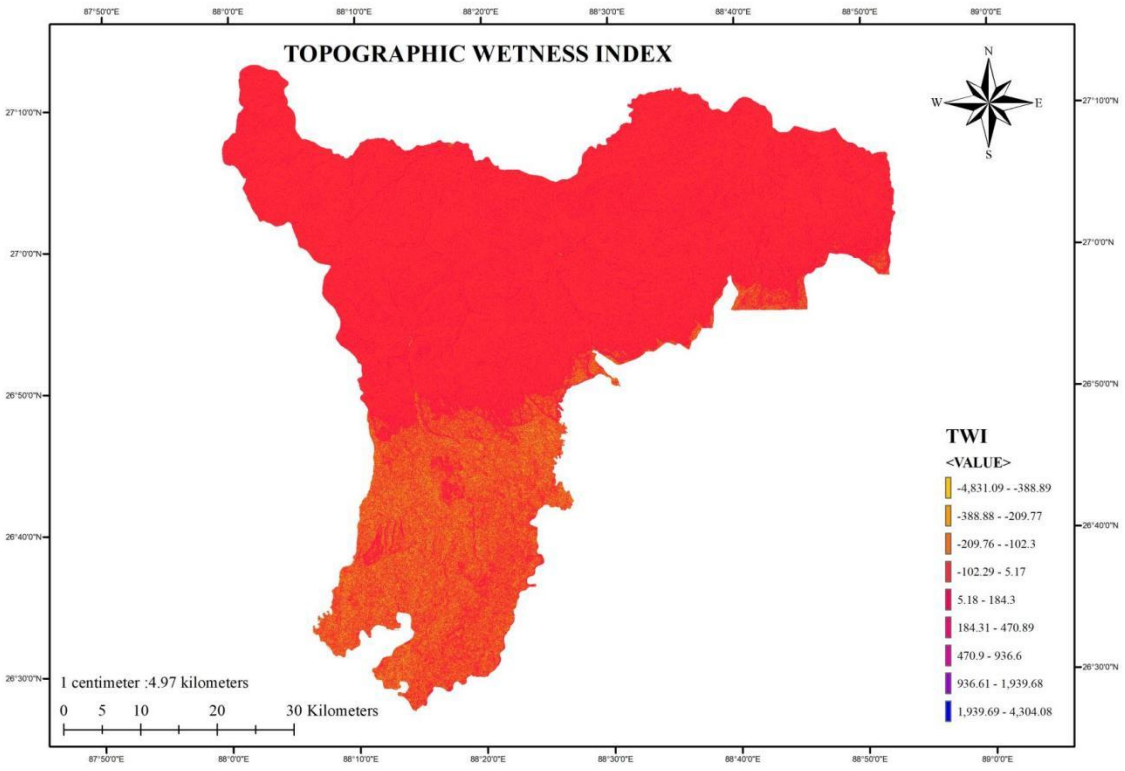

Fig 4.6 Topographic Wetness Index (TWI) map

4.3.6 Stream Power Index:

The Digital Elevation Model (DEM) is used to calculate the Stream Power Index (SPI), a derivative that measures the erosional power of streams. In order to identify regions with greater stream power, it takes into account variables like slope and flow accumulation. SPI assists in identifying locations where streams have a stronger propensity to erode and destabilise slopes, suggesting probable landslide-prone zones, in landslide susceptibility mapping. Due to stream erosion and changes in slope stability conditions, higher SPI values indicate a greater sensitivity to landslides.

SPI can be calculated mathematically as:

SPI= Ln (Flow Accumulation+0.001) * ((Slope in Percentage/100)+0.001))

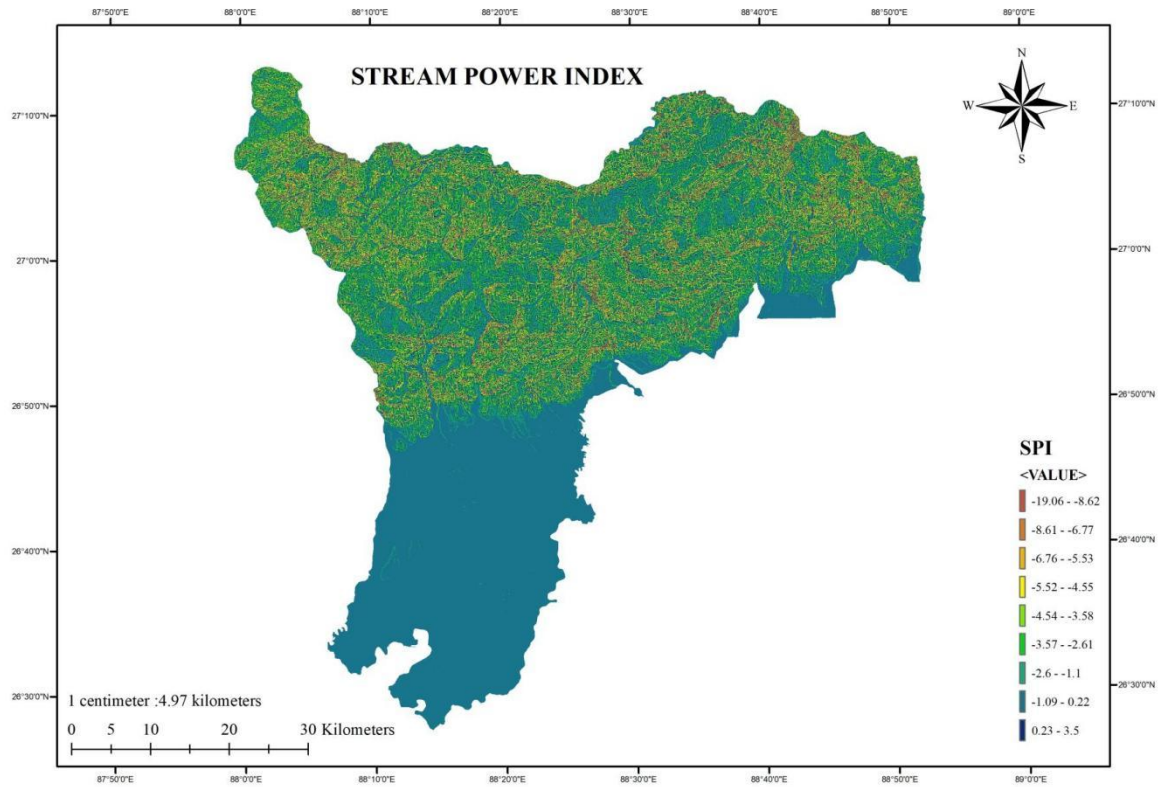

Fig 4.7 Stream Power Index (SPI) map

4.4 Thematic Layers:

4.4.1 Distance to Roads:

In landslip susceptibility mapping, the distance to roads is a conditioning factor that quantifies a location's closeness to road networks. It offers useful details on people's activities, accessibility, and potential annoyances brought on by road construction and maintenance. Due to things like slope change, soil disturbance, and higher human-induced activity, areas closer to roadways may show increased landslip susceptibility. When prioritising management and mitigation techniques, distance to roadways helps identify regions where manmade effects and related factors may contribute to the incidence of landslides.

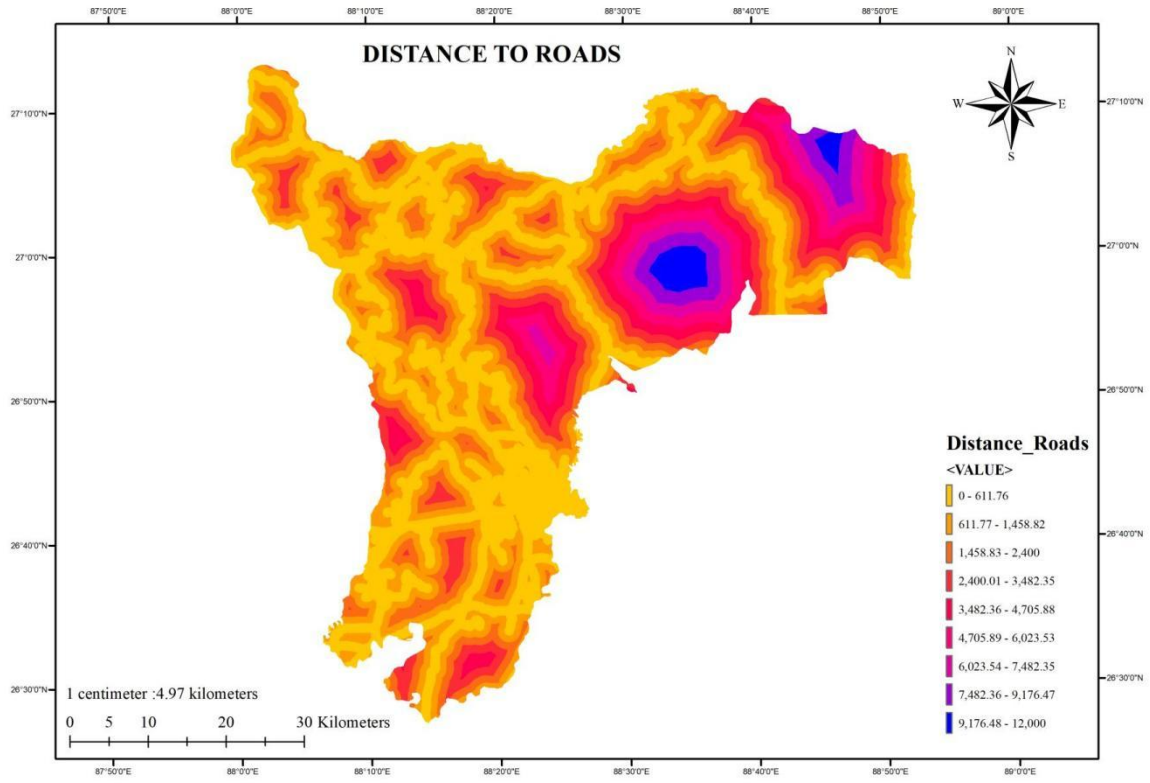

Fig. 4.8 Distance to roads map

4.4.2 Distance to Rivers:

When calculating landslip susceptibility maps, distance to rivers is a crucial conditioning factor that quantifies a location's closeness to river networks. Regarding hydrological processes and how they affect slope stability, it offers useful information. Due to elements including water erosion, slope undercutting, and changes in groundwater levels, areas near to rivers may be more prone to landslides. The ability to pinpoint regions where fluvial processes may cause slope instability and to prioritise management and mitigation activities is made possible by the presence of rivers. Understanding the relationship between watercourses and potentially landslide-prone locations is improved by analysing the distance to rivers.

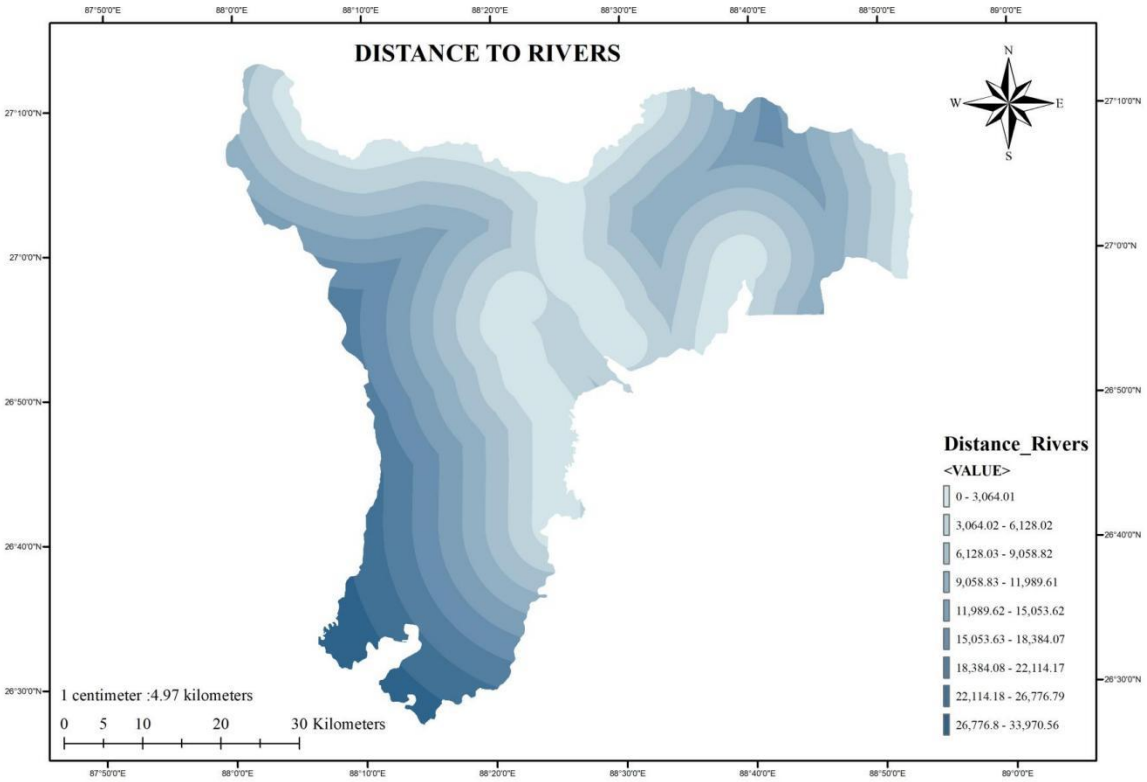

Fig. 4.9 Distance to rivers map

4.4.3 Distance to Faults/Lineaments:

The proximity of sites to linear features, such as faults, fractures, or geological lineaments, is measured by a conditioning factor called distance to lineaments, which is employed in landslip susceptibility mapping. Lineaments can act as favoured routes for the flow of groundwater or other geologic processes as well as function as indicators of potential structural vulnerabilities in the landscape. Due to the impact of structural elements, areas closer to lineaments may show increased sensitivity to landslides. It is possible to identify regions where geological characteristics can contribute to slope instability and prioritise them for additional analysis and mitigation actions by taking the distance to lineaments into account.

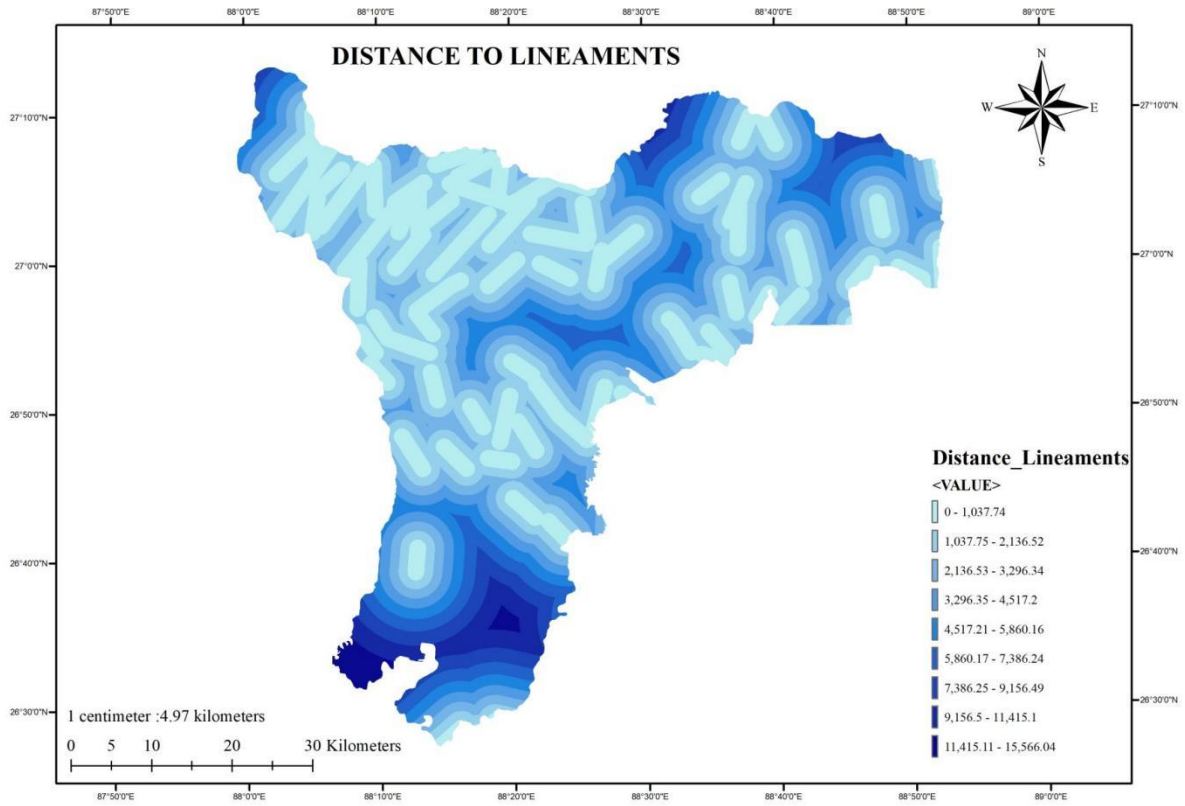

Fig. 4.10 Distance to faults/lineaments map

4.4.4 Lithology:

The geological makeup and characteristics of the underlying rock or soil elements in a certain area are characterised by lithology, a significant conditioning factor utilised in landslip susceptibility mapping. Slope stability may be impacted by differences in the strength, cohesiveness, and permeability of various lithological units. Higher landslip susceptibility is frequently linked to specific lithologies, such as weak or worn rocks, clay-rich formations, or unconsolidated deposits. To help in the assessment and management of landslide hazards, it is feasible to identify regions with particular geological formations that are more prone to landslides by taking lithology into account.

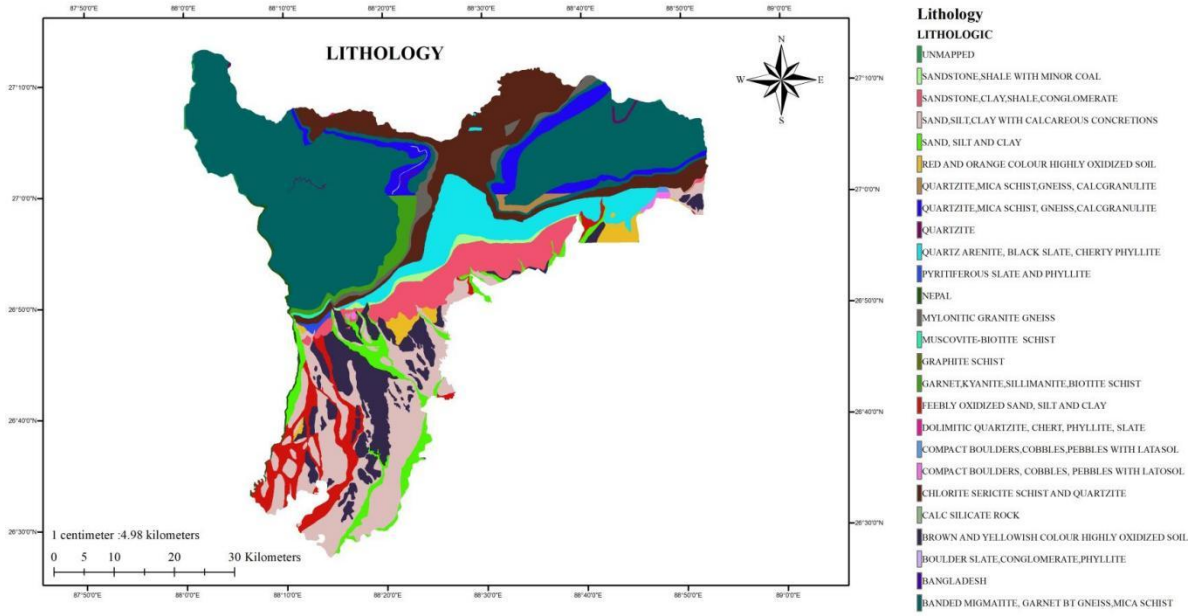

Figure 4.11 Lithology Map

4.4.5 Geology:

Geology, which includes the study of the Earth's solid components like rocks, minerals, and geological formations, is a crucial conditioning element utilised in landslip susceptibility mapping. It offers significant new understandings of the underlying geological mechanisms and structural characteristics that can affect slope stability. Different geological units have unique characteristics that affect landslip occurrence, such as rock strength, susceptibility to weathering, and structural features. It is possible to identify locations with certain geological formations that are more prone to landslides by taking into account the composition and structure of the local geology. This helps with the assessment, mapping, and management of landslide hazards.

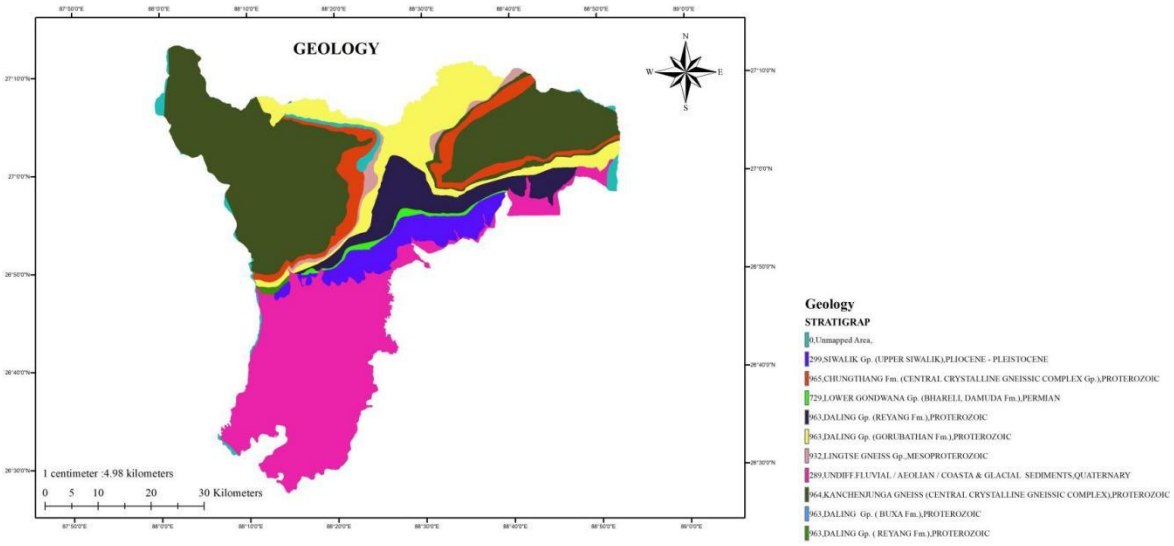

Figure 4.12 Geology Map

4.4.6 Land Use Land Cover:

Land Use/Land Cover (LULC) describes the distribution and characteristics of various land cover types and land use activities in a specific area and is a crucial conditioning element utilised in landslip susceptibility mapping. The spatial patterns of vegetation, urban areas, farms, woods, bare soil, and other land cover categories can all be better understood using LULC data. Through elements including root reinforcement, surface runoff, surface roughness, and human-induced alterations, different land cover types can affect slope stability. Landslides may be more likely to occur in specific land cover types, such as steep slopes with little vegetation or regions with heavy human activity. It is possible to locate regions where particular land cover types contribute to the occurrence of landslides and to prioritise management efforts to reduce landslide risks by taking into account LULC in landslide susceptibility mapping.

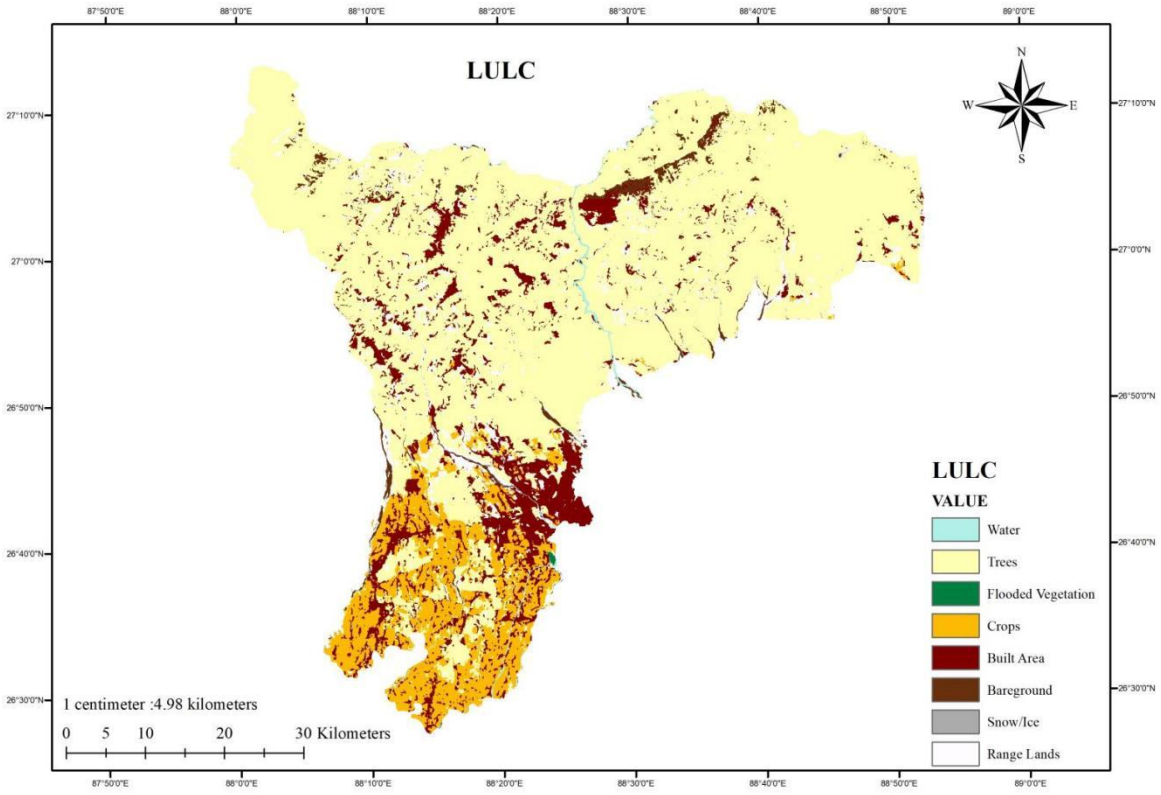

Figure 4.13 LULC Map

4.4.7 Rainfall:

When determining a region's susceptibility to landslides, rainfall is a significant conditioning factor that measures the volume and intensity of precipitation there. By penetrating the soil, raising pore water pressure, and weakening slopes' shear strength, it significantly contributes to the start of landslides. Due to increased soil saturation and decreased slope stability, areas that receive more rainfall or have strong rainstorm events are more likely to experience landslides. It is possible to identify places with higher rainfall volumes or intensities that are more susceptible to the occurrence of landslides by including rainfall data into landslide susceptibility mapping. This facilitates the assessment and mitigation of landslide hazards.

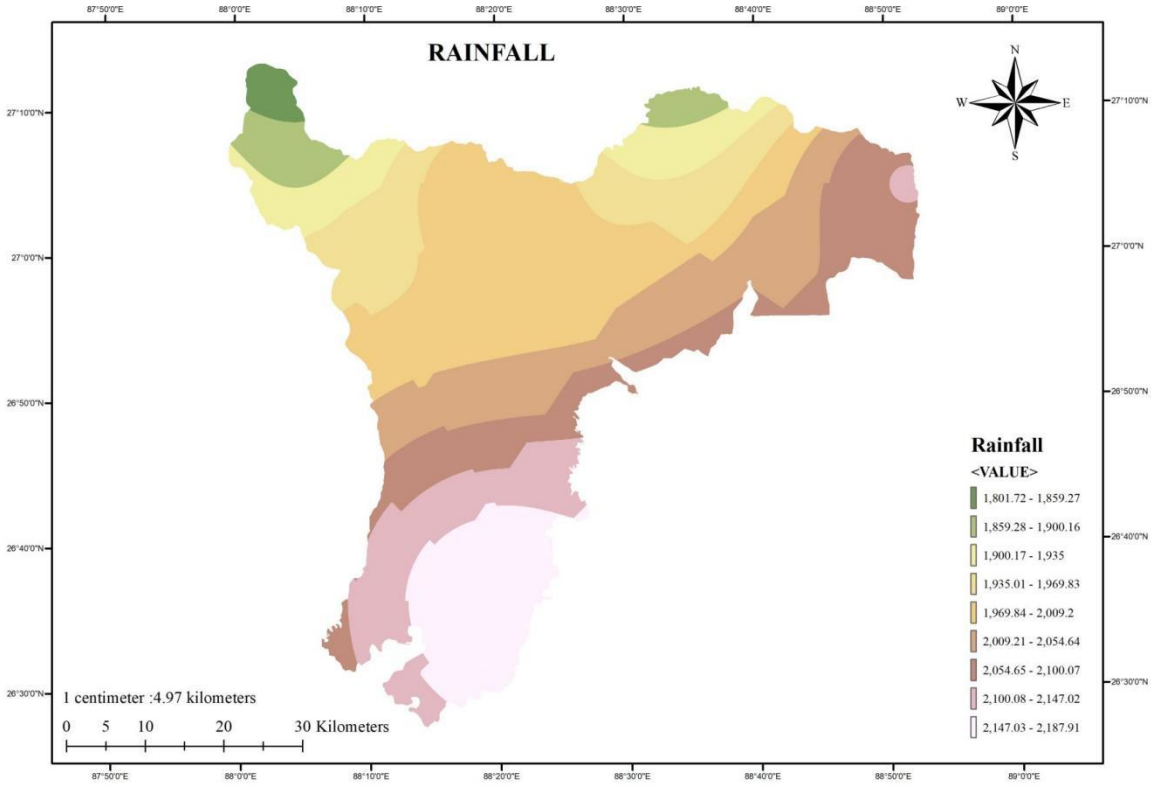

Figure 4.14 Rainfall Map

4.5 Landslide Inventory Map:

The locations and extents of previous landslip events within a specific area are identified and delineated on a landslip inventory map, which is a geospatial depiction. It is made by methodically compiling and analysing data from a variety of sources, such as field surveys, remote sensing photography, aerial photographs, historical records, and expert knowledge. The inventory map offers important details regarding the research area's landslides' spatial distribution, frequency, magnitude, and other features. As a result of enabling the link between conditioning elements and previous landslip events, it serves as a basis for mapping landslip susceptibility. The inventory map makes it easier to comprehend spatial patterns and spot high-risk locations that are vulnerable to landslides, which makes it easier to plan for effective land use and to detect hazards and develop mitigation measures.

In this instance, the landslide inventory was obtained in point shapefile format from the Bhukosh portal of the Geological Survey of India, and 300 landslide points were selected for the purpose of landslide susceptibility mapping.

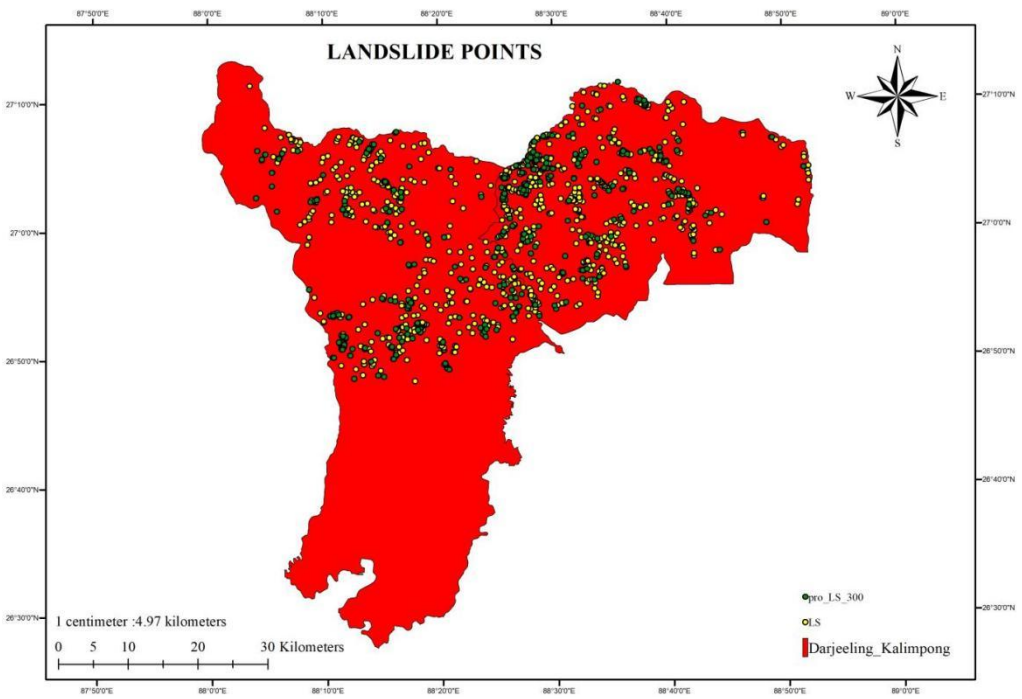

Figure 4.15 Landslides Points Map

4.5.1 Random Splitting of Samples:

Landslip susceptibility mapping frequently use the random splitting of samples technique to split the dataset into training and validation subsets. It entails arbitrarily dividing the available landslip data into two distinct groups, often with a predetermined ratio, such as 80% for training and 20% for validation/testing. Out of the 300 points that were collected for the landslip inventory, 80% were collected for the training dataset and the remaining 20% were collected for the testing dataset.

The following steps are involved in the process of randomly splitting samples:

Data collection and preparation: Compiling information on landslides and the relevant conditioning variables, such as slope, height, land cover, etc., that are employed in the study.

Random Partitioning: Each landslip data point is randomly assigned to either the training subset or the testing subset using random partitioning. This prevents bias or overfitting in the model and guarantees a fair representation of landslides in both subsets.

Training Subset: The landslip susceptibility model is developed using the training subset. The model can learn and recognise patterns, correlations, and dependencies between the conditioning factors and landslip events because it has the majority of the landslip data.

Testing Subset: The generated model's performance and accuracy are evaluated using the testing subset, which is made up of the remaining landslip data. It is used as a separate dataset to assess the prediction power and generalizability of the model.

The resulting landslip susceptibility model can be improved by randomly dividing the samples into training and testing subsets. When applied to new regions or potential landslip events, it aids in evaluating the model's performance on unobserved data and provides an estimate of its prediction accuracy.

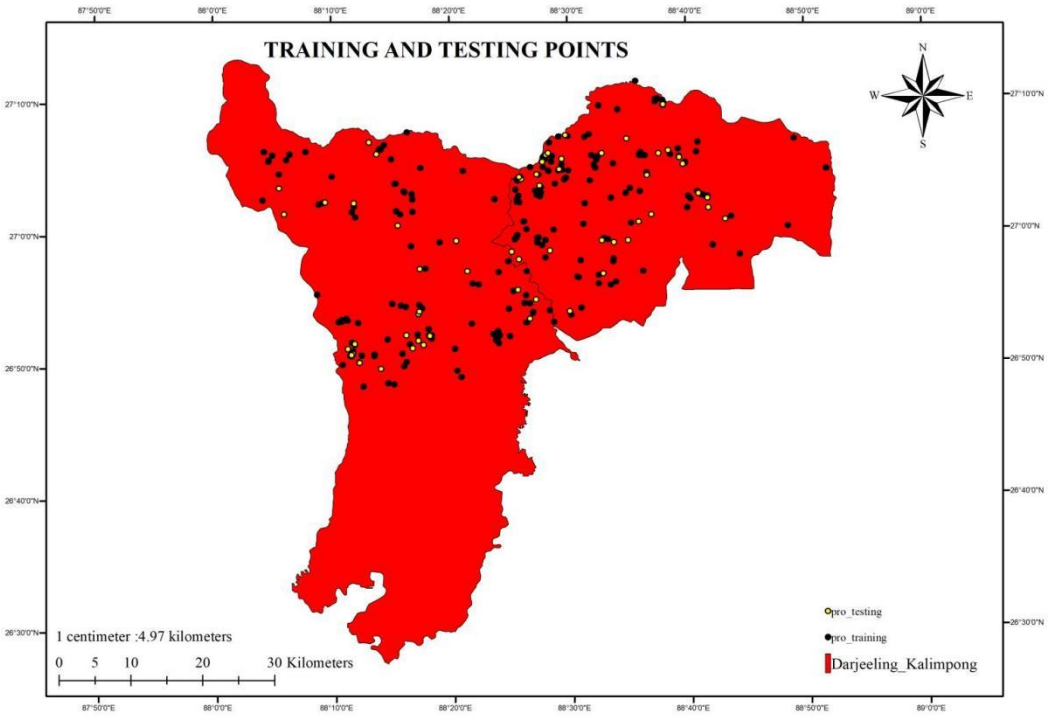

Figure 4.16 Training and Testing Data

CHAPTER 5 - ADOPTED PROBABILITY APPROACHES: CONCEPTS AND COMPUTATION RESULTS

5.1 Statistical methods incorporated in the study:

The study uses a variety of statistical techniques to model and analyse landslip susceptibility. These techniques offer a quantitative framework for analysing the connections between environmental conditions and the occurrence of landslides. The following statistical techniques were used in the study:

Shannon Entropy (SE): The measure of disorder or variability in the distribution of landslip events across several classes of conditioning factors is called Shannon Entropy (SE). It measures the information gained by taking a certain factor into account and aids in the discovery of factors with greater discriminating power.

Weight-of-Evidence (WOE): The Weight-of-Evidence technique (WOE) assesses the likelihood of a landslip occurring for each class of a conditioning factor in comparison to a reference class. By calculating the odds ratio and allocating weights to each class, it is possible to identify the variables that increase or decrease landslip susceptibility.

Statistical Index Method (SIM): The Statistical Index Method (SIM) analyses statistical indices including mean, standard deviation, and correlation coefficients to quantify the relationship between conditioning factors and landslides. It helps to understand the influences on landslide susceptibility of elements that differ significantly between landslide and non-landslide locations.

In order to build a solid landslip susceptibility model, these statistical tools help quantify the correlations between the conditioning elements and landslip occurrences. The project seeks to improve the precision and dependability of the landslide susceptibility mapping process through the integration of various methodologies, allowing for a better identification and prioritisation of landslide-prone areas for efficient land management and hazard mitigation tactics.

5.1.1 Shannon's Entropy:

In order to measure the information content or variability in the distribution of landslip occurrences across several classes of conditioning factors, Shannon's entropy is a statistical technique used in landslip susceptibility mapping. It evaluates the data's diversity or disorder and aids in the discovery of variables with more discriminatory potential for landslip susceptibility. The importance of these factors on the occurrence of landslides is highlighted by higher entropy values, which show a more diverse distribution of landslides across factor classes.

The following is the mathematical formulation for the above technique:

$$E = -k \sum RF * Log (RF) \quad (5.1)$$

$$W_i = \frac{1-E}{\sum(1-E)} \quad (5.2)$$

Where, k = 1/ Log (m), E = Entropy, m = Number of classes in factor, W_i = Weights of every factor, i = activating factors

The LSM can be produced in ArcGIS by using a raster calculator after performing the aforementioned calculations in the Excel sheet as follows:

$$LSM = \sum (Weights * FR_{maps}) \quad (5.3)$$

Table 5.1 displays the computation of Shannon's Entropy for each factor.

Table 5.1. Result for every factor using Shannon's Entropy

ELEVATION	**FACTOR CLASS**	**LANDSLIDE PIXELS**	**CLASS PIXELS**	**FR**	**RF**	**RF*logRF**
	62 - 456	36900	1286460	0.478	0.097	-0.098
	456.01 - 1007	62100	773055	1.338	0.272	-0.154
	1007.01 - 1592	69300	701039	1.646	0.335	-0.159
	1592.01 - 2312	36900	495313	1.241	0.252	-0.151
	2312.01 - 3616	2700	206291	0.218	0.044	-0.060
		207900	3462158	4.920	1.000	-0.622
SLOPE	**FACTOR CLASS**	**LANDSLIDE PIXELS**	**CLASS PIXELS**	**FR**	**RF**	**RF*logRF**
	0 - 5.91	0	996006	0.000	0.000	0.000
	5.92 - 13.23	10800	209542	0.862	0.070	-0.081
	13.24 - 18.86	14400	320938	0.751	0.061	-0.074
	18.87 - 23.65	31500	426810	1.235	0.101	-0.100
	23.66 - 28.15	40500	456553	1.484	0.121	-0.111
	28.16 - 32.93	36900	425801	1.450	0.118	-0.110
	32.94 - 38	32400	334433	1.621	0.132	-0.116
	38.01 - 44.76	28800	207274	2.325	0.190	-0.137
	44.77 - 71.78	10800	71444	2.530	0.206	-0.141
		206100	3448801	12.259	1.000	-0.871
CURVATURE	**FACTOR CLASS**	**LANDSLIDE PIXELS**	**CLASS PIXELS**	**FR**	**RF**	**RF*logRF**
	-37.22 - -6.9	3600	13092	4.619	0.325	-0.159
	-6.89 - -3.86	5400	89187	1.017	0.071	-0.082
	-3.85 - -1.97	27900	289020	1.622	0.114	-0.108
	-1.96 - -0.83	61200	703070	1.462	0.103	-0.102
	-0.82 - -0.07	47700	1438882	0.557	0.039	-0.055
	-0.06 - 1.07	41400	583270	1.192	0.084	-0.090
	1.08 - 2.96	12600	267777	0.790	0.056	-0.070
	2.97 - 5.99	5400	68420	1.326	0.093	-0.096
	6 - 59.44	900	9219	1.640	0.115	-0.108
		206100	3461937	14.225	1.000	-0.869
ASPECT	**FACTOR CLASS**	**LANDSLIDE PIXELS**	**CLASS PIXELS**	**FR**	**RF**	**RF*logRF**
	Flat (-1)	12600	305016	0.688249198	0.07061587 5	-0.081285768
	North (0 - 22.5)	20700	330489	1.043544868	0.10706998	-0.10389346

					8	2
	North-East (22.5 - 67.5)	30600	399512	1.2761 1375	0.130 93206 5	- 0.11560698 8
	East (67.5 - 112.5)	33300	427742	1.2970 60184	0.133 08121 5	- 0.11656360 6
	South-East (112.5 - 157.5)	27900	419791	1.1073 09103	0.113 61233 9	- 0.10731531 8
	South (1575 - 202.5)	18900	335416	0.9388 05919	0.096 32354 3	- 0.09789049 1
	South-West (202.5 - 247.5)	18900	354727	0.8876 98219	0.091 07978 1	- 0.09477561 8
	West (247.5 - 292.5)	18900	297776	1.0574 74498	0.108 49919 9	- 0.10465544 9
	North-West (292.5 - 337.5)	16200	290457	0.9292 4655	0.095 34273 1	- 0.09731750 9
	North (337.5 - 360)	9000	287875	0.5208 78401	0.053 44326 4	- 0.06798555 2
		207000	3448801	9.746	1	-0.987
SPI	**FACTOR CLASS**	**LANDSLIDE PIXELS**	**CLASS PIXELS**	**FR**	**RF**	**RF*logRF**
	-19.06 - -8.62	2700	5938	7.576	0.391	-0.159
	-8.61 - -6.77	2700	31496	1.428	0.074	-0.083
	-6.76 - -5.53	16200	92816	2.908	0.150	-0.124
	-5.52 - -4.55	19800	182822	1.804	0.093	-0.096
	-4.54 - -3.58	27000	309777	1.452	0.075	-0.084
	-3.57 - -2.61	28800	340081	1.411	0.073	-0.083
	-2.60 - -1.1	16200	243250	1.110	0.057	-0.071
	-1.09 - 0.22	38700	1519406	0.424	0.022	-0.036
	0.23 - 3.5	54900	723215	1.265	0.065	-0.077
		207000	3448801	19.378	1.000	-0.815
TWI	**FACTOR CLASS**	**LANDSLIDE PIXELS**	**CLASS PIXELS**	**FR**	**RF**	**RF*logRF**
	-4831.09 - -388.89	0	23616	0.000	0.000	0.000
	-388.88 - -209.77	0	149449	0.000	0.000	0.000
	-209.76 - -102.3	0	298847	0.000	0.000	0.000
	-102.29 - 5.17	39600	691143	0.955	0.430	-0.158
	5.18 - 184.3	167400	2203673	1.266	0.570	-0.139
	184.31 - 470.89	0	66898	0.000	0.000	0.000
	470.9 - 936.6	0	12235	0.000	0.000	0.000

	936.61 - 1939.68	0	2663	0.000	0.000	0.000
	1939.69 - 4304.08	0	277	0.000	0.000	0.000
		207000	3448801	2.220	1.000	-0.297
DISTANCE TO ROADS	**FACTOR CLASS**	**LANDSLIDE PIXELS**	**CLASS PIXELS**	**FR**	**RF**	**RF*logRF**
	0 - 611.76	117000	1039105	1.883	0.244	-0.150
	611.77 - 1458.82	18000	753355	0.400	0.052	-0.067
	1458.83 - 2400	18900	556372	0.568	0.074	-0.083
	2400.01 - 3482.35	22500	380486	0.989	0.128	-0.114
	3482.36 - 4705.88	6300	250035	0.421	0.055	-0.069
	4705.89 - 6023.53	9000	183001	0.823	0.107	-0.104
	6023.54 - 7482.35	7200	138483	0.870	0.113	-0.107
	7482.36 - 9176.47	4500	102147	0.737	0.096	-0.097
	9176.48 - 12000	3600	58953	1.021	0.132	-0.116
		207000	3461937	7.711	1.000	-0.907
DISTANCE TO LINEAMENTS	**FACTOR CLASS**	**LANDSLIDE PIXELS**	**CLASS PIXELS**	**FR**	**RF**	**RF*logRF**
	0 - 1037.74	44100	728581	1.008	0.149	-0.123
	1037.75 - 2136.52	40500	715578	0.942	0.140	-0.119
	2136.53 - 3296.34	45900	581469	1.314	0.195	-0.138
	3296.35 - 4517.20	44100	457116	1.606	0.238	-0.148
	4517.21 - 5860.16	18000	389391	0.770	0.114	-0.108
	5860.17 - 7386.24	11700	260974	0.747	0.111	-0.106
	7386.25 - 9156.49	3600	167291	0.358	0.053	-0.068
	9156.50 - 11415.10	0	117553	0.000	0.000	0.000
	11415.11 - 15566.04	0	43889	0.000	0.000	0.000
		207900	3461842	6.746	1.000	-0.811
DISTANCE TO RIVERS	**FACTOR CLASS**	**LANDSLIDE PIXELS**	**CLASS PIXELS**	**FR**	**RF**	**RF*logRF**
	0 - 3064.01	44100	629279	1.167	0.176	-0.133
	3064.02 - 6128.02	57600	730452	1.313	0.198	-0.139
	6128.03 - 9058.82	36900	593103	1.036	0.156	-0.126
	9058.83 - 11989.61	38700	530802	1.214	0.183	-0.135
	11989.62 - 15053.62	11700	345952	0.563	0.085	-0.091
	15053.63 -	17100	242928	1.172	0.177	-0.133

	18384.07					
	18384.08 - 22114.17	1800	189453	0.158	0.024	-0.039
	22114.18 - 26776.79	0	118152	0.000	0.000	0.000
	26776.80 - 33970.56	0	81721	0.000	0.000	0.000
		207900	3461842	6.623	1.000	-0.796
RAINFALL	**FACTOR CLASS**	**LANDSLIDE PIXELS**	**CLASS PIXELS**	**FR**	**RF**	**RF*logRF**
	1801.72 - 1859.27	0	44723	0.000	0.000	0.000
	1859.28 - 1900.16	12600	133705	1.569	0.206	-0.141
	1900.17 - 1935	12600	233549	0.898	0.118	-0.110
	1935.01 - 1969.83	44100	394792	1.860	0.244	-0.150
	1969.84 - 2009.20	83700	909668	1.532	0.201	-0.140
	2009.21 - 2054.64	50400	534876	1.569	0.206	-0.141
	2054.65 - 2100.07	2700	471960	0.095	0.013	-0.024
	2100.08 - 2147.02	1800	349351	0.086	0.011	-0.022
	2147.03 - 2187.91	0	389218	0.000	0.000	0.000
		207900	3461842	7.610	1.000	-0.728
GEOLOGY	**FACTOR CLASS**	**LANDSLIDE PIXELS**	**CLASS PIXELS**	**FR**	**RF**	**RF*logRF**
	NULL	0	58179	0	0	0
	PLEISTOCENE	13500	196726	1.142680353	0.0902131104	-0.09424837
	PROTEROZOIC	10800	204953	0.877449698	0.0692734944	-0.080317969
	PERMIAN	3600	28266	2.120756952	0.1674309599	-0.129953922
	PROTEROZOIC (R)	27900	244589	1.899415751	0.1499563633	-0.123569307
	PROTEROZOIC (G)	56700	398724	2.367900421	0.1869426009	-0.136148751
	MESOPROTEROZOIC	2700	46070	0.975884242	0.0770447711	-0.085770618
	QUATERNARY	3600	1024024	0.058538976	0.0046215715	-0.010792348
	PROTEROZOIC (C)	88200	1252788	1.172313466	0.0925525599	-0.09566342
	PROTEROZOIC (B)	0	218	0	0	0

	PROTEROZOIC (R)	900	7305	2.051516633	0.16196452	-0.128045931
		207900	3461842	12.666	1	-0.885
LULC	**FACTOR CLASS**	**LANDSLIDE PIXELS**	**CLASS PIXELS**	**FR**	**RF**	**RF*logRF**
	WATER	200	194153	1.389	0.167	-0.130
	TREES	15400	21892621	0.949	0.114	-0.107
	FLOODED VEGETATION	0	10430	0.000	0.000	0.000
	CROPS	0	3437288	0.000	0.000	0.000
	BUILT AREA	4900	3350392	1.973	0.237	-0.148
	BAREGROUND	1300	589670	2.974	0.357	-0.160
	SNOW	0	4135	0.000	0.000	0.000
	RANGE LANDS	1300	1678346	1.045	0.125	-0.113
		23100	31157035	8.329	1.000	-0.658
LITHOLOGY	**FACTOR CLASS**	**LANDSLIDE PIXELS**	**CLASS PIXELS**	**FR**	**RF**	**RF*logRF**
	NULL	900	451316	0.033	0.001	-0.004
	SANDSTONE, SHALE WITH MINOR COAL	1800	119593	0.250	0.009	-0.019
	SANDSTONE,CLAY,SHALE,CONGLOMERATE	0	130	0.000	0.000	0.000
	SAND,SILT,CLAY WITH CALCAREOUS CONCRETIONS	0	146491	0.000	0.000	0.000
	SAND, SILT AND CLAY	900	16797	0.891	0.033	-0.049
	RED AND ORANGE COLOUR HIGHLY OXIDIZED SOIL	0	47715	0.000	0.000	0.000
	QUARTZITE, MICA SCHIST;GNEISS, CALCGRANULITE	0	258855	0.000	0.000	0.000
	QUARTZITE, MICA SCHIST;GNEISS, CALCGRANULITE	28800	245007	1.956	0.073	-0.083
	QUARTZITE	0	6833	0.000	0.000	0.000

	QUARTZ ARENITE, BLACK SLATE, CHERTY PHYLLITE	900	1718	8.716	0.327	-0.159
	PYRITIFEROUS SLATE AND PHYLLITE	54000	394135	2.280	0.085	-0.091
	NEPAL	3600	28974	2.067	0.078	-0.086
	MYLONITIC GRANITE GNEISS	13500	199152	1.128	0.042	-0.058
	MUSCOVITE-BIOTITE SCHIST	86400	1265544	1.136	0.043	-0.058
	GRAPHITE SCHIST	0	15092	0.000	0.000	0.000
	GARNET.KYANITE,SILLIMANITE, BIOTITE SCHIST	2700	53561	0.839	0.031	-0.047
	FEEBLY OXIDIZED SAND, SILT AND CLAY	4500	49877	1.501	0.056	-0.070
	DOLIMITIC QUARTZITE, CHERT, PHYLLITE, SLATE	900	6367	2.352	0.088	-0.093
	COMPACT BOULDERS COBBLES PEBBLES WITH LATOSOL	900	5953	2.515	0.094	-0.097
	COMPACT BOULDERS, COBBLES, PEBBLES WITH LATOSOL	0	3758	0.000	0.000	0.000
	CHLORITE SERICITE SCHIST AND QUARTZITE	0	228	0.000	0.000	0.000
	CALC SILICATE ROCK	8100	134183	1.004	0.038	-0.054
	BROWN AND YELLOWISH COLOUR HIGHLY OXIDIZED SOIL	0	5571	0.000	0.000	0.000
	BOULDER SLATE. CONGLOMERATE, PHYLLITE	0	359	0.000	0.000	0.000

	BANGLADESH	0	1745	0.000	0.000	0.000
	BANDED MIGMATITE, GARNET BT GNEISS,MICA	0	5	0.000	0.000	0.000
		207900	3458959	26.668	1.000	-0.969

Table 5.2 provides the calculation and weights for Shannon's Entropy.

Table 5.2. Weights for every factor using Shannon's Entropy

CAUSATIVE FACTOR	m	k	Ej	1 - Ej	Wi
ELEVATION	5	1.431	0.8899	0.1101	0.0445
SLOPE	9	1.048	0.9128	0.0872	0.0352
CURVATURE	9	1.048	0.9106	0.0894	0.0361
ASPECT	10	1.000	0.9873	0.0127	0.0051
SPI	9	1.048	0.8536	0.1464	0.0592
TWI	9	1.048	0.3110	0.6890	0.2784
ROADS	9	1.048	0.9507	0.0493	0.0199
LINEAMENTS	9	1.048	0.8495	0.1505	0.0608
RIVERS	9	1.048	0.8343	0.1657	0.0670
RAINFALL	9	1.048	0.7627	0.2373	0.0959
GEOLOGY	11	0.960	0.8494	0.1506	0.0609
LULC	8	1.107	0.7288	0.2712	0.1096
LITHOLOGY	26	0.707	0.6846	0.3154	0.1274
			10.525	2.475	1

5.1.2 Statistical Index Method:

When assessing the association between conditioning factors and landslip occurrences, the Statistical Index Method (SIM), a statistical technique, is applied. With this technique, the significance and impact of each conditioning element on landslip susceptibility are quantified by examining numerous statistical indices.

The goal of the study is to pinpoint the conditioning elements that significantly affect landslip susceptibility by using the statistical index method. Understanding the connections between these elements and landslides, enhancing the precision and dependability of landslide susceptibility models, and assisting decision-making in land use planning and landslide hazard mitigation activities are all made easier with the use of this knowledge.

The weight calculation equation is as follows:

$$SI = \ln [(N_L/N_C)/(N_{TL}/N_{CL})] \quad (5.4)$$

where,

N_{CL} = the map's overall pixel

N_{TL} = total pixel with landslides

N_C = class pixel

N_L = landslides pixels in class

The LSM can be determined in ArcGIS by using the Raster Calculator as follows after performing the aforementioned calculations in the Excel sheet:

$$LSM = \sum (SIM_{maps}) \quad (5.5)$$

Table 5.3 displays the statistical indices computation result for all the factors.

Table 5.3. Result of Statistical Indices for every activating factor

	FACTOR CLASS	LANDSLIDE PIXELS	CLASS PIXELS	SI
ELEVATION	62 - 456	36900	1286460	-0.739
	456.01 - 1007	62100	773055	0.291
	1007.01 - 1592	69300	701039	0.498
	1592.01 - 2312	36900	495313	0.216
	2312.01 - 3616	2700	206291	-1.523
		207900	3462158	-1.257
SLOPE	**FACTOR CLASS**	**LANDSLIDE PIXELS**	**CLASS PIXELS**	**SI**
	0 - 5.91	0	996006	0.000
	5.92 - 13.23	10800	209542	-0.148
	13.24 - 18.86	14400	320938	-0.287
	18.87 - 23.65	31500	426810	0.211
	23.66 - 28.15	40500	456553	0.395
	28.16 - 32.93	36900	425801	0.372
	32.94 - 38	32400	334433	0.483
	38.01 - 44.76	28800	207274	0.844
	44.77 - 71.78	10800	71444	0.928
		206100	3448801	2.798
CURVATURE	**FACTOR CLASS**	**LANDSLIDE PIXELS**	**CLASS PIXELS**	**SI**
	-37.22 - -6.9	3600	13092	1.530
	-6.89 - -3.86	5400	89187	0.017
	-3.85 - -1.97	27900	289020	0.483
	-1.96 - -0.83	61200	703070	0.380
	-0.82 - -0.07	47700	1438882	-0.585
	-0.06 - 1.07	41400	583270	0.176
	1.08 - 2.96	12600	267777	-0.235
	2.97 - 5.99	5400	68420	0.282
	6 - 59.44	900	9219	0.495
		206100	3461937	2.542
ASPECT	**FACTOR CLASS**	**LANDSLIDE PIXELS**	**CLASS PIXELS**	**SI**
	Flat (-1)	12600	305016	-0.374
	North (0 - 22.5)	20700	330489	0.043
	North-East (22.5 - 67.5)	30600	399512	0.244
	East (67.5 - 112.5)	33300	427742	0.260

	South-East (112.5 - 157.5)	27900	419791	0.102
	South (1575 - 202.5)	18900	335416	-0.063
	South-West (202.5 - 247.5)	18900	354727	-0.119
	West (247.5 - 292.5)	18900	297776	0.056
	North-West (292.5 - 337.5)	16200	290457	-0.073
	North (337.5 - 360)	9000	287875	-0.652
		207000	3448801	-0.577
SPI	**FACTOR CLASS**	**LANDSLIDE PIXELS**	**CLASS PIXELS**	**SI**
	-19.06 - -8.62	2700	5938	2.025
	-8.61 - -6.77	2700	31496	0.356
	-6.76 - -5.53	16200	92816	1.067
	-5.52 - -4.55	19800	182822	0.590
	-4.54 - -3.58	27000	309777	0.373
	-3.57 - -2.61	28800	340081	0.344
	-2.60 - -1.1	16200	243250	0.104
	-1.09 - 0.22	38700	1519406	-0.857
	0.23 - 3.5	54900	723215	0.235
		207000	3448801	4.238
TWI	**FACTOR CLASS**	**LANDSLIDE PIXELS**	**CLASS PIXELS**	**SI**
	-4831.09 - -388.89	0	23616	0.000
	-388.88 - -209.77	0	149449	0.000
	-209.76 - -102.3	0	298847	0.000
	-102.29 - 5.17	39600	691143	-0.046
	5.18 - 184.3	167400	2203673	0.236
	184.31 - 470.89	0	66898	0.000
	470.9 - 936.6	0	12235	0.000
	936.61 - 1939.68	0	2663	0.000
	1939.69 - 4304.08	0	277	0.000
		207000	3448801	0.189
DISTANCE TO ROADS	**FACTOR CLASS**	**LANDSLIDE PIXELS**	**CLASS PIXELS**	**SI**
	0 - 611.76	117000	1039105	0.633

	611.77 - 1458.82	18000	753355	-0.917
	1458.83 - 2400	18900	556372	-0.565
	2400.01 - 3482.35	22500	380486	-0.011
	3482.36 - 4705.88	6300	250035	-0.864
	4705.89 - 6023.53	9000	183001	-0.195
	6023.54 - 7482.35	7200	138483	-0.140
	7482.36 - 9176.47	4500	102147	-0.305
	9176.48 - 12000	3600	58953	0.021
		207000	3461937	-2.345
DISTANCE TO LINEAMENTS	**FACTOR CLASS**	**LANDSLIDE PIXELS**	**CLASS PIXELS**	**SI**
	0 - 1037.74	44100	728581	0.008
	1037.75 - 2136.52	40500	715578	-0.059
	2136.53 - 3296.34	45900	581469	0.273
	3296.35 - 4517.20	44100	457116	0.474
	4517.21 - 5860.16	18000	389391	-0.262
	5860.17 - 7386.24	11700	260974	-0.292
	7386.25 - 9156.49	3600	167291	-1.026
	9156.50 - 11415.10	0	117553	0.000
	11415.11 - 15566.04	0	43889	0.000
		207900	3461842	-0.884
DISTANCE TO RIVERS	**FACTOR CLASS**	**LANDSLIDE PIXELS**	**CLASS PIXELS**	**SI**
	0 - 3064.01	44100	629279	0.154
	3064.02 - 6128.02	57600	730452	0.272
	6128.03 - 9058.82	36900	593103	0.035
	9058.83 - 11989.61	38700	530802	0.194
	11989.62 - 15053.62	11700	345952	-0.574
	15053.63 - 18384.07	17100	242928	0.159
	18384.08 - 22114.17	1800	189453	-1.844
	22114.18 - 26776.79	0	118152	0.000
	26776.80 - 33970.56	0	81721	0.000
		207900	3461842	-1.603

	FACTOR CLASS	LANDSLIDE PIXELS	CLASS PIXELS	SI
RAINFALL	1801.72 - 1859.27	0	44723	0.000
	1859.28 - 1900.16	12600	133705	0.451
	1900.17 - 1935	12600	233549	-0.107
	1935.01 - 1969.83	44100	394792	0.621
	1969.84 - 2009.20	83700	909668	0.427
	2009.21 - 2054.64	50400	534876	0.450
	2054.65 - 2100.07	2700	471960	-2.351
	2100.08 - 2147.02	1800	349351	-2.456
	2147.03 - 2187.91	0	389218	0.000
		207900	3461842	-2.966
GEOLOGY	**FACTOR CLASS**	**LANDSLIDE PIXELS**	**CLASS PIXELS**	**SI**
	NULL	0	58179	0.000
	PLEISTOCENE	13500	196726	0.136
	PROTEROZOIC	10800	204953	-0.129
	PERMIAN	3600	28266	0.754
	PROTEROZOIC (R)	27900	244589	0.644
	PROTEROZOIC (G)	56700	398724	0.864
	MESOPROTEROZOIC	2700	46070	-0.022
	QUATERNARY	3600	1024024	-2.836
	PROTEROZOIC (C)	88200	1252788	0.161
	PROTEROZOIC (B)	0	218	0.000
	PROTEROZOIC (R)	900	7305	0.721
		207900	3461842	0.293
LULC	**FACTOR CLASS**	**LANDSLIDE PIXELS**	**CLASS PIXELS**	**SI**
	WATER	200	194153	0.329
	TREES	15400	21892621	-0.053
	FLOODED VEGETATION	0	10430	0.000
	CROPS	0	3437288	0.000
	BUILT AREA	4900	3350392	0.679
	BAREGROUND	1300	589670	1.090

	SNOW	0	4135	0.000
	RANGE LANDS	1300	1678346	0.044
		23100	31157035	2.089
	FACTOR CLASS	**LANDSLIDE PIXELS**	**CLASS PIXELS**	**SI**
LITHOLOGY	NULL	900	451316	-3.406
	SANDSTONE, SHALE WITH MINOR COAL	1800	119593	-1.385
	SANDSTONE, CLAY,SHALE, CONGLOMERATE	0	130	0.000
	SAND,SILT,CLAY WITH CALCAREOUS CONCRETIONS	0	146491	0.000
	SAND, SILT AND CLAY	900	16797	-0.115
	RED AND ORANGE COLOUR HIGHLY OXIDIZED SOIL	0	47715	0.000
	QUARTZITE, MICA SCHIST;GNEISS, CALCGRANULITE	0	258855	0.000
	QUARTZITE, MICA SCHIST;GNEISS, CALCGRANULITE	28800	245007	0.671
	QUARTZITE	0	6833	0.000
	QUARTZ ARENITE, BLACK SLATE, CHERTY PHYLLITE	900	1718	2.165
	PYRITIFEROUS SLATE AND PHYLLITE	54000	394135	0.824
	NEPAL	3600	28974	0.726
	MYLONITIC GRANITE GNEISS	13500	199152	0.120
	MUSCOVITE-BIOTITE SCHIST	86400	1265544	0.127

	GRAPHITE SCHIST	0	15092	0.000
	GARNET.KYANITE,SILLIMANITE, BIOTITE SCHIST	2700	53561	-0.176
	FEEBLY OXIDIZED SAND, SILT AND CLAY	4500	49877	0.406
	DOLIMITIC QUARTZITE, CHERT, PHYLLITE, SLATE	900	6367	0.855
	COMPACT BOULDERS COBBLES PEBBLES WITH LATOSOL	900	5953	0.922
	COMPACT BOULDERS, COBBLES, PEBBLES WITH LATOSOL	0	3758	0.000
	CHLORITE SERICITE SCHIST AND QUARTZITE	0	228	0.000
	CALC SILICATE ROCK	8100	134183	0.004
	BROWN AND YELLOWISH COLOUR HIGHLY OXIDIZED SOIL	0	5571	0.000
	BOULDER SLATE. CONGLOMERATE, PHYLLITE	0	359	0.000
	BANGLADESH	0	1745	0.000
	BANDED MIGMATITE, GARNET BT GNEISS,MICA	0	5	0.000
		207900	3458959	1.741

5.1.3 Weight of Evidence:

A statistical technique called Weight of Evidence (WOE) is frequently used in landslide susceptibility mapping to assess the likelihood of landslides occurring for various classes of conditioning factors. In comparison to a reference class, it measures the magnitude and direction of the association between each factor class and landslip susceptibility.

The natural logarithm of the ratio of the proportion of landslides in a given factor class to the proportion of landslides in the reference class is used to compute the WOE. A higher likelihood of a landslip than the reference class is indicated by a positive WOE value, whilst a lesser likelihood is indicated by a negative value.

Each factor class is given weights according to the WOE approach based on its WOE value. These weights represent how each component class contributes most to landslip vulnerability. Higher weighted factors are thought to have a greater impact on landslip occurrence.

The study intends to identify and prioritise the component classes that have a stronger association with landslip vulnerability by using the Weight of Evidence technique. The landslip susceptibility model can be improved upon using this data, leading to increased predictive power. Additionally, the WOE analysis weights can be utilised to build a weighted overlay technique, in which the variables are blended according to their individual weights to provide a composite map of landslip susceptibility.

Some quantities must be determined for calculating purposes. the following values:

$$N_1 = N_L$$

$$N_2 = N_{TL} - N_L$$

$$N_3 = N_C - N_L$$

$$N_4 = N_{CL} - N_{TL} - N_C + N_L$$

$$W^{+} = \ln \frac{\frac{N_1}{N_1 + N_2}}{\frac{N_3}{N_3 + N_4}} \quad (5.6)$$

$$W^{-} = \ln \frac{\frac{N_2}{N_1 + N_2}}{\frac{N_4}{N_3 + N_4}} \quad (5.7)$$

where,

N_1 = pixels of landslide on a factor class,

N_2 = pixels of landslide absent from a factor class,

N_3 = pixels in a particular factor class that do not include any pixels from landslides and class

N_4 = pixels where the provided factor and the landslide are absent

N_{CL} = the map's overall pixel

N_{TL} = total pixel with landslides

N_C = class pixel

N_L = landslides pixels in class

To determine the extent of C for the specified vulnerability variable, these values are used.

$$C = W^{+} - W^{-} \quad (5.8)$$

where,

C = contrast value

W^{+} = weight allocated to a certain raster indicating the impact of a factor class

W^{-} = weight allocated under the absence of factor class

The positive value of C indicates a high likelihood of occurrence, whereas the negative value indicates a lower likelihood.

The LSM can be determined in ArcGIS using the Raster Calculator after performing the aforementioned calculations in the Excel sheet as follows:

$$LSM = \sum (C_{maps}) \quad (5.9)$$

Table 5.4 displays the computation for Weight of Evidence for each factor.

Table 5.4. Result of Weight of Evidence for every activating factor

	FACTOR CLASS	LANDSLIDE PIXELS	CLASS PIXELS	W+	W-	C
ELEVATION	62 - 456	36900	1286460	-0.772	0.289	-1.061
	456.01 - 1007	62100	773055	0.313	-0.108	0.421
	1007.01 - 1592	69300	701039	0.541	-0.190	0.730
	1592.01 - 2312	36900	495313	0.231	-0.044	0.275
	2312.01 - 3616	2700	206291	-1.572	0.052	-1.624
		207900	3462158			
	FACTOR CLASS	**LANDSLIDE PIXELS**	**CLASS PIXELS**	**W+**	**W-**	**C**
SLOPE	0 - 5.91	0	996006	0.000	0.367	-0.367
	5.92 - 13.23	10800	209542	-0.157	0.009	-0.166
	13.24 - 18.86	14400	320938	-0.302	0.027	-0.329
	18.87 - 23.65	31500	426810	0.226	-0.036	0.262
	23.66 - 28.15	40500	456553	0.426	-0.081	0.508
	28.16 - 32.93	36900	425801	0.401	-0.070	0.470
	32.94 - 38	32400	334433	0.523	-0.073	0.597
	38.01 - 44.76	28800	207274	0.932	-0.094	1.026
	44.77 - 71.78	10800	71444	1.030	-0.035	1.065
		206100	3448801			
	FACTOR CLASS	**LANDSLIDE PIXELS**	**CLASS PIXELS**	**W+**	**W-**	**C**
CURVATURE	-37.22 - -6.9	3600	13092	1.790	-0.015	1.805
	-6.89 - -3.86	5400	89187	0.018	0.000	0.018
	-3.85 - -1.97	27900	289020	0.523	-0.062	0.585
	-1.96 - -0.83	61200	703070	0.410	-0.133	0.542
	-0.82 - -0.07	47700	1438882	-0.613	0.294	-0.907
	-0.06 - 1.07	41400	583270	0.188	-0.042	0.230
	1.08 - 2.96	12600	267777	-0.248	0.019	-0.267
	2.97 - 5.99	5400	68420	0.303	-0.007	0.310
	6 - 59.44	900	9219	0.536	-0.002	0.538
		206100	3461937			
	FACTOR CLASS	**LANDSLIDE PIXELS**	**CLASS PIXELS**	**W+**	**W-**	**C**
ASPECT	Flat (-1)	12600	305016	-0.393	0.032	-0.425
	North (0 - 22.5)	20700	330489	0.045	-0.005	0.050

	North-East (22.5 - 67.5)	30600	399512	0.262	-0.039	0.301
	East (67.5 - 112.5)	33300	427742	0.279	-0.046	0.325
	South-East (112.5 - 157.5)	27900	419791	0.109	-0.016	0.125
	South (1575 - 202.5)	18900	335416	-0.067	0.007	-0.074
	South-West (202.5 - 247.5)	18900	354727	-0.126	0.014	-0.140
	West (247.5 - 292.5)	18900	297776	0.060	-0.006	0.065
	North-West (292.5 - 337.5)	16200	290457	-0.078	0.007	-0.085
	North (337.5 - 360)	9000	287875	-0.682	0.045	-0.728
		207000	3448801			
SPI	**FACTOR CLASS**	**LANDSLIDE PIXELS**	**CLASS PIXELS**	**W+**	**W-**	**C**
	-19.06 - -8.62	2700	5938	2.569	-0.012	2.582
	-8.61 - -6.77	2700	31496	0.384	-0.004	0.388
	-6.76 - -5.53	16200	92816	1.197	-0.058	1.255
	-5.52 - -4.55	19800	182822	0.643	-0.049	0.692
	-4.54 - -3.58	27000	309777	0.402	-0.048	0.451
	-3.57 - -2.61	28800	340081	0.371	-0.049	0.420
	-2.60 - -1.1	16200	243250	0.111	-0.009	0.120
	-1.09 - 0.22	38700	1519406	-0.893	0.403	-1.296
	0.23 - 3.5	54900	723215	0.252	-0.077	0.329
		207000	3448801			
TWI	**FACTOR CLASS**	**LANDSLIDE PIXELS**	**CLASS PIXELS**	**W+**	**W-**	**C**
	-4831.09 - -388.89	0	23616	0.000	0.007	-0.007
	-388.88 - -209.77	0	149449	0.000	0.047	-0.047
	-209.76 - -102.3	0	298847	0.000	0.097	-0.097
	-102.29 - 5.17	39600	691143	-0.049	0.012	-0.061
	5.18 - 184.3	167400	2203673	0.253	-0.665	0.917
	184.31 - 470.89	0	66898	0.000	0.021	-0.021
	470.9 - 936.6	0	12235	0.000	0.004	-0.004
	936.61 - 1939.68	0	2663	0.000	0.001	-0.001
	1939.69 - 4304.08	0	277	0.000	0.000	0.000
		207000	3448801			

	FACTOR CLASS	LANDSLIDE PIXELS	CLASS PIXELS	W+	W-	C
DISTANCE TO ROADS	0 - 611.76	117000	1039105	0.691	-0.500	1.191
	611.77 - 1458.82	18000	753355	-0.955	0.165	-1.120
	1458.83 - 2400	18900	556372	-0.593	0.085	-0.677
	2400.01 - 3482.35	22500	380486	-0.012	0.001	-0.013
	3482.36 - 4705.88	6300	250035	-0.900	0.047	-0.947
	4705.89 - 6023.53	9000	183001	-0.207	0.010	-0.217
	6023.54 - 7482.35	7200	138483	-0.148	0.006	-0.154
	7482.36 - 9176.47	4500	102147	-0.322	0.008	-0.331
	9176.48 - 12000	3600	58953	0.022	0.000	0.023
		207000	3461937			
DISTANCE TO LINEAMENTS	FACTOR CLASS	LANDSLIDE PIXELS	CLASS PIXELS	W+	W-	C
	0 - 1037.74	44100	728581	0.008	-0.002	0.011
	1037.75 - 2136.52	40500	715578	-0.063	0.016	-0.079
	2136.53 - 3296.34	45900	581469	0.294	-0.070	0.363
	3296.35 - 4517.20	44100	457116	0.514	-0.103	0.616
	4517.21 - 5860.16	18000	389391	-0.276	0.031	-0.307
	5860.17 - 7386.24	11700	260974	-0.308	0.022	-0.330
	7386.25 - 9156.49	3600	167291	-1.066	0.034	-1.101
	9156.50 - 11415.10	0	117553	0.000	0.037	-0.037
	11415.11 - 15566.04	0	43889	0.000	0.014	-0.014
		207900	3461842			
DISTANCE TO RIVERS	FACTOR CLASS	LANDSLIDE PIXELS	CLASS PIXELS	W+	W-	C
	0 - 3064.01	44100	629279	0.165	-0.040	0.205
	3064.02 - 6128.02	57600	730452	0.293	-0.093	0.385
	6128.03 - 9058.82	36900	593103	0.038	-0.008	0.046
	9058.83 - 11989.61	38700	530802	0.208	-0.042	0.250
	11989.62 - 15053.62	11700	345952	-0.602	0.050	-0.652
	15053.63 - 18384.07	17100	242928	0.170	-0.014	0.184
	18384.08 - 22114.17	1800	189453	-1.896	0.051	-1.947

	22114.18 - 26776.79	0	118152	0.000	0.037	-0.037
	26776.80 - 33970.56	0	81721	0.000	0.025	-0.025
		207900	3461842			
RAINFALL	**FACTOR CLASS**	**LANDSLIDE PIXELS**	**CLASS PIXELS**	**W+**	**W-**	**C**
	1801.72 - 1859.27	0	44723	0.000	0.014	-0.014
	1859.28 - 1900.16	12600	133705	0.488	-0.025	0.512
	1900.17 - 1935	12600	233549	-0.114	0.008	-0.121
	1935.01 - 1969.83	44100	394792	0.677	-0.124	0.801
	1969.84 - 2009.20	83700	909668	0.461	-0.222	0.684
	2009.21 - 2054.64	50400	534876	0.487	-0.116	0.604
	2054.65 - 2100.07	2700	471960	-2.407	0.143	-2.550
	2100.08 - 2147.02	1800	349351	-2.513	0.104	-2.617
	2147.03 - 2187.91	0	389218	0.000	0.127	-0.127
		207900	3461842			
GEOLOGY	**FACTOR CLASS**	**LANDSLIDE PIXELS**	**CLASS PIXELS**	**W+**	**W-**	**C**
	NULL	0	58179	0.000	0.018	-0.018
	PLEISTOCENE	13500	196726	0.145	-0.009	0.154
	PROTEROZOIC	10800	204953	-0.136	0.008	-0.144
	PERMIAN	3600	28266	0.828	-0.010	0.838
	PROTEROZOIC (R)	27900	244589	0.703	-0.076	0.779
	PROTEROZOIC (G)	56700	398724	0.956	-0.209	1.165
	MESOPROTEROZOIC	2700	46070	-0.024	0.000	-0.024
	QUATERNARY	3600	1024024	-2.894	0.360	-3.254
	PROTEROZOIC (C)	88200	1252788	0.172	-0.111	0.283
	PROTEROZOIC (B)	0	218	0.000	0.000	0.000
	PROTEROZOIC (R)	900	7305	0.790	-0.002	0.793
		207900	3461842			
LULC	**FACTOR CLASS**	**LANDSLIDE PIXELS**	**CLASS PIXELS**	**W+**	**W-**	**C**
	WATER	200	194153	0.329	-0.002	0.332
	TREES	15400	21892621	-0.053	0.114	-0.167
	FLOODED	0	10430	0.000	0.000	0.000

	VEGETATION					
	CROPS	0	3437288	0.000	0.117	-0.117
	BUILT AREA	4900	3350392	0.680	-0.125	0.805
	BAREGROUND	1300	589670	1.091	-0.039	1.130
	SNOW	0	4135	0.000	0.000	0.000
	RANGE LANDS	1300	1678346	0.044	-0.003	0.046
		23100	31157035			
LITHOLOGY	**FACTOR CLASS**	**LANDSLIDE PIXELS**	**CLASS PIXELS**	**W+**	**W-**	**C**
	NULL	900	451316	-3.466	0.145	-3.611
	SANDSTONE, SHALE WITH MINOR COAL	1800	119593	-1.431	0.028	-1.460
	SANDSTONE, CLAY,SHALE, CONGLOMERATE	0	130	0.000	0.000	0.000
	SAND,SILT,CLAY WITH CALCAREOUS CONCRETIONS	0	146491	0.000	0.046	-0.046
	SAND, SILT AND CLAY	900	16797	-0.122	0.001	-0.122
	RED AND ORANGE COLOUR HIGHLY OXIDIZED SOIL	0	47715	0.000	0.015	-0.015
	QUARTZITE, MICA SCHIST;GNEISS, CALCGRANULITE	0	258855	0.000	0.083	-0.083
	QUARTZITE, MICA SCHIST;GNEISS, CALCGRANULITE	28800	245007	0.734	-0.080	0.814
	QUARTZITE	0	6833	0.000	0.002	-0.002
	QUARTZ ARENITE, BLACK SLATE, CHERTY PHYLLITE	900	1718	2.845	-0.004	2.849
	PYRITIFEROUS SLATE AND PHYLLITE	54000	394135	0.909	-0.190	1.100

	NEPAL	3600	28974	0.797	-0.010	0.807
	MYLONITIC GRANITE GNEISS	13500	199152	0.128	-0.008	0.137
	MUSCOVITE-BIOTITE SCHIST	86400	1265544	0.136	-0.087	0.223
	GRAPHITE SCHIST	0	15092	0.000	0.005	-0.005
	GARNET.KYANITE,SILLIMANITE, BIOTITE SCHIST	2700	53561	-0.186	0.003	-0.189
	FEEBLY OXIDIZED SAND, SILT AND CLAY	4500	49877	0.439	-0.008	0.447
	DOLIMITIC QUARTZITE, CHERT, PHYLLITE, SLATE	900	6367	0.946	-0.003	0.948
	COMPACT BOULDERS COBBLES PEBBLES WITH LATOSOL	900	5953	1.024	-0.003	1.027
	COMPACT BOULDERS, COBBLES, PEBBLES WITH LATOSOL	0	3758	0.000	0.001	-0.001
	CHLORITE SERICITE SCHIST AND QUARTZITE	0	228	0.000	0.000	0.000
	CALC SILICATE ROCK	8100	134183	0.005	0.000	0.005
	BROWN AND YELLOWISH COLOUR HIGHLY OXIDIZED SOIL	0	5571	0.000	0.002	-0.002
	BOULDER SLATE. CONGLOMERATE, PHYLLITE	0	359	0.000	0.000	0.000
	BANGLADESH	0	1745	0.000	0.001	-0.001
	BANDED MIGMATITE, GARNET BT GNEISS,MICA	0	5	0.000	0.000	0.000
		207900	3458959			

CHAPTER 6 - RESULTS AND DISCUSSIONS

6.1 Landslide Susceptibility Map (LSM) Generation and Classification:

The data from the three methods—Shannon's Entropy (SE), Statistical Index Method (SIM), and Weight of Evidence (WoE)—were combined to create Landslide Susceptibility Mapping (LSM). The LSM sought to divide the research region into distinct susceptibility zones using the information gathered from each of these approaches.

The results of SE, SIM, and WoE were integrated using the appropriate ensemble approach or weighted overlay analysis to get the LSM. The resulting LSM highlighted locations with varied degrees of susceptibility and showed the geographical distribution of landslip susceptibility throughout the research area.

The LSM was then categorised using a categorization scheme into various susceptibility classifications. To determine distinct thresholds for categorising the LSM into useful groups, natural breaks or comparable statistical techniques were used. Typically, classification was done using five susceptibility classes, such as very low, low, moderate, high, and very high.

Based on its matching susceptibility value, the classification procedure assigned each cell or pixel in the LSM to a particular susceptibility class. This categorization made it possible to visualise and comprehend the patterns of landslip susceptibility throughout the research area in great detail.

Planning for the development of infrastructure, catastrophe risk reduction, and land use all benefit from the generated LSM and its classification. The LSM can be used by decision-makers and stakeholders to prioritise mitigation strategies, carry out focused initiatives, and lessen the potential impact of landslides in the zones with high and very high susceptibility.

6.1.1 Analysis of Landslide Susceptibility using Probabilistic Approaches:

Table 6.1. Region-wise distribution of landslide and class area

	LANDSLIDE SUSCEPTIBILITY CLASS	LANDSLIDE AREA	LANDSLIDE AREA (%)	CLASS AREA	CLASS AREA (%)
SE	VERY LOW	0	0	302590	8.781
	LOW	0	0	251316	7.293
	MODERATE	2700	1.304	376456	10.924
	HIGH	33300	16.087	830748	24.107
	VERY HIGH	171000	82.609	1684919	48.895
		207000	100	3446029	100
	LANDSLIDE SUSCEPTIBILITY CLASS	**LANDSLIDE AREA**	**LANDSLIDE AREA (%)**	**CLASS AREA**	**CLASS AREA (%)**
SIM	VERY LOW	0	0	423157	12.280
	LOW	900	0.435	551679	16.009
	MODERATE	9000	4.348	448333	13.010
	HIGH	38700	18.696	1120329	32.511
	VERY HIGH	158400	76.522	902531	26.190
		207000	100	3446029	100
	LANDSLIDE SUSCEPTIBILITY CLASS	**LANDSLIDE AREA**	**LANDSLIDE AREA (%)**	**CLASS AREA**	**CLASS AREA (%)**
WoE	VERY LOW	0	0	480871	13.954
	LOW	900	0.435	525192	15.240
	MODERATE	9900	4.783	506206	14.690
	HIGH	50400	24.348	1121526	32.545
	VERY HIGH	145800	70.435	812234	23.570
		207000	100	3446029	100

The following conclusions were added after analysing landslip susceptibility using Shanon's Entropy (SE), the Statistical Index Method (SIM), and the weight of Evidence (WoE):

Shannon's Entropy (SE): The study area was divided into five susceptibility groups for the SE-based landslip vulnerability map. No landslides were seen in the classes with extremely low and low susceptibility, which made up 8.781% and 7.293% of the research region, respectively. The high and very high susceptibility classes covered 16.087% and 82.609% of the total landslip area, respectively, while the moderate susceptibility class made up 1.304% of that area.

Statistical Index Method (SIM): SIM-based analysis showed that the study region covered

12.280% of the extremely low susceptibility class, with no landslides being reported. The moderate, high, and very high susceptibility classes accounted for 4.348%, 18.696%, and 76.522% of the total landslide area, respectively, whereas the low susceptibility class made for 0.435% of the overall landslide area.

The study area was divided into five susceptibility groups depending on the weight of the evidence (WoE) in the analysis. 13.954% of the research area was in the very low class, where there were no landslides seen. The moderate, high, and very high susceptibility classes accounted for 4.783%, 24.348%, and 70.435% of the total landslide area, respectively, whereas the low susceptibility class made for 0.435% of the overall landslide area.

Based on the unique criteria for each approach, the categorization results offer useful insights into the amount and distribution of landslip susceptibility throughout the study area.

6.2 Landslide Susceptibility Map (LSM):

6.2.1 Shanon’s Entropy (SE):

The mapping of the subject area's vulnerability to landslides using Shannon's Entropy approach provided insightful information about the importance and role of conditioning factors. With the help of this method, it was possible to quantify the amount of information and variability in the distribution of landslip occurrences among various factor classes. The proportionate weights of each factor in determining landslip susceptibility were determined by allocating weights to the factor classes based on their entropy values.

According to the analysis, the factor class of Topographic Wetness Index (TWI) was given about 28% of the overall weights, showing that it has a significant impact on the likelihood of landslides. This shows that TWI is essential in establishing how landslides are distributed spatially in the studied area. The overall landslip susceptibility was influenced by factors like lithology and land use and land cover (LULC), which had weights of about 13% and 11%, respectively.

Additionally, a composite susceptibility map was created using the weights acquired from the

Shannon's Entropy approach, incorporating the contributions of each element. The map displayed five classifications of landslip susceptibility in terms of spatial representation: very low, low, moderate, high, and very high. The findings showed that places with heightened landslip risk made up 73% of the entire study area, falling into the high and very high susceptibility groups. On the other hand, low and very low susceptibility were present in 73% of the area, indicating moderately stable terrain.

It is crucial to keep in mind that the weights obtained from the Shannon's Entropy approach offer a comparative indicator of factor relevance within the research domain. However, to ensure a thorough understanding of the regional landslip dynamics, their interpretation should be done in conjunction with field observations and professional knowledge.

In conclusion, Shannon's Entropy method has demonstrated to be a successful way for landslip susceptibility mapping in the research area. This method quantifies the information content and assigns weights to factor classes. The findings highlight the key elements and offer useful data for decision-making, hazard reduction, and land use planning.

The Landslide Susceptibility Map for Shanon’s Entropy is depicted below in Fig. 6.1.

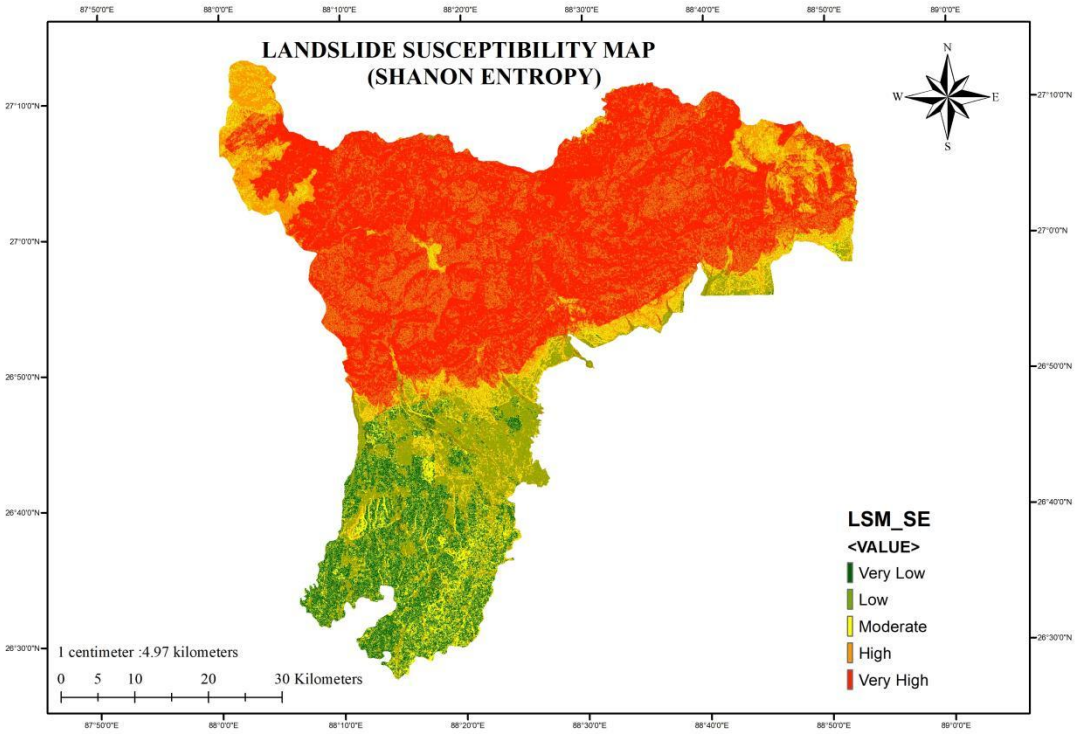

Fig. 6.1 Landslide Susceptibility Map for Shanon’s Entropy (SE) model

6.2.2 Statistical Index Method (SIM):

In order to evaluate the prediction ability and contribution of each conditioning element in landslip susceptibility mapping, the Statistical Index Method (SIM) method was used. In order to indicate the elements' relative importance in the susceptibility modelling process, this method ranks the factors according to their information gain.

According to the investigation, the Statistical Index Method of the Stream Power Index (SPI) was 4.238, showing that the SPI has a high degree of predictability and makes a considerable contribution to the occurrence of landslides. A similar SI value of 2.798 was seen for Slope, indicating its significance in the susceptibility mapping procedure. In order to understand the individual contributions of other parameters like curvature and lithology, the SI values of those components were also computed.

The most significant influencing elements for landslip susceptibility can be found by ranking conditioning factors according to their Statistical Index Method. These variables are essential for comprehending how landslides are distributed spatially and can help with efficient land use planning and hazard management.

It is crucial to remember that the Statistical Index Method should be interpreted in conjunction with field observations and subject-matter expertise. Although the SI technique offers insightful information about the relative significance of conditioning elements, it is important to be aware of its drawbacks and presumptions. To improve the precision of the susceptibility mapping, it may be necessary to do additional research and make adjustments on variables like rainfall and distance to roads.

In summary, the Statistical Index Method (SIM) technique was used in the study region to rank conditioning factors according to their ability to predict landslip vulnerability. The susceptibility mapping process is made easier to understand in terms of relative relevance thanks to the Statistical Index Method analysis, which also makes judgements more accurate and trustworthy. These results support sensible land use planning and lessen the danger of landslides in the study area.

The Landslide Susceptibility Map for Shanon's Entropy is depicted below in Fig. 6.2.

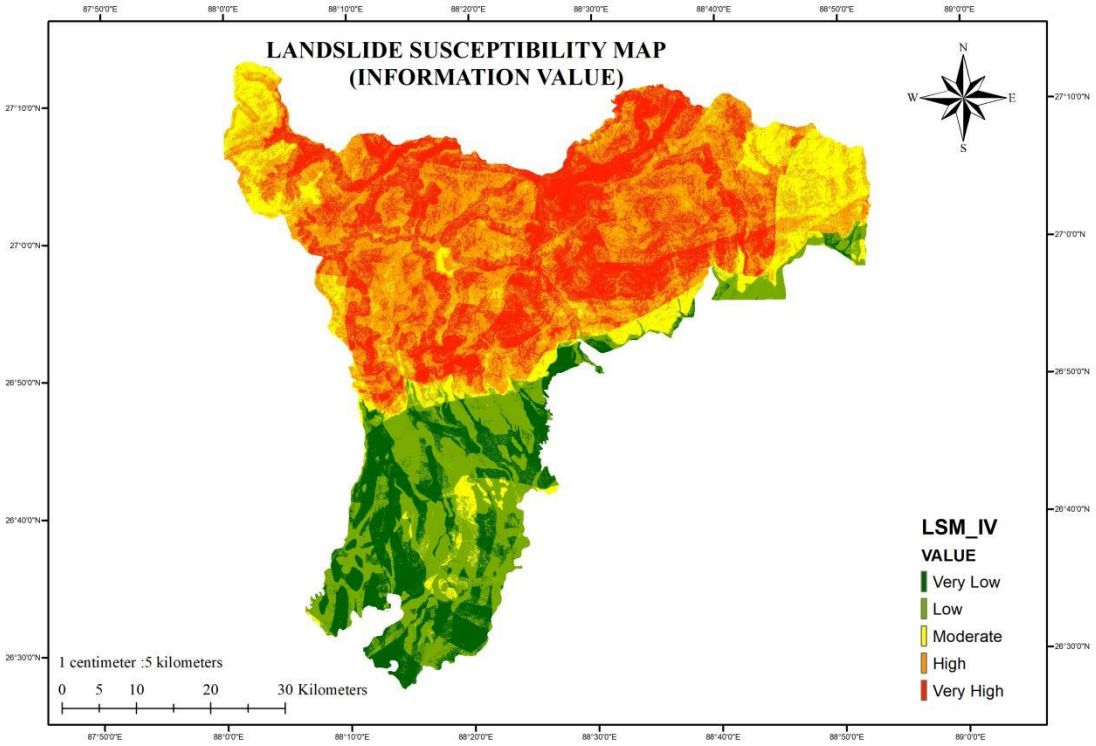

Fig. 6.2 Landslide Susceptibility Map for Statistical Index Method (SIM) model

6.2.3 Weight of Evidence (WoE):

To determine the possibility of a landslip occurring in the research area of Darjeeling and Kalimpong, the Weight of Evidence (WoE) technique was used. The method assisted in determining the contrast value (C) for each class of conditioning elements to help predict the likelihood of landslides. A lesser probability was represented by negative C values, whilst a higher probability was indicated by positive values. The analysis showed that a number of factors increased the likelihood of landslides in the Darjeeling Kalimpong area, including elevations between 1008 and 1592 metres, slopes between 23.66 and 28.15 degrees, curvatures between -37.22 and -6.9, SPIs between 19.06 and 8.62, TWIs between 5.18 and 184.3, distances from rivers between 3064.02 and 6128.02 metres, distances from roads between 0 and 611. Figure 6.3's vulnerability map, which was created using the Weight of Evidence technique, gives a visual picture of the study area's various levels of landslip

susceptibility.

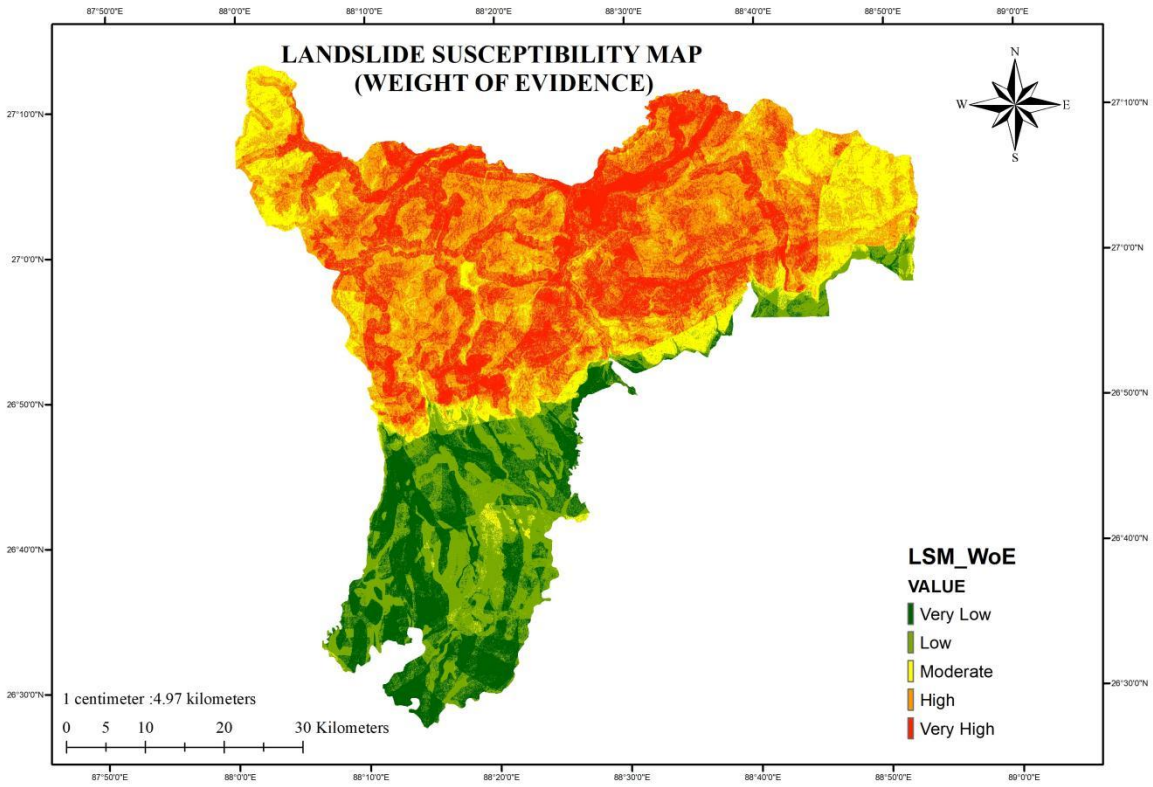

Fig. 6.3 Landslide Susceptibility Map for Weight of Evidence (WoE) model

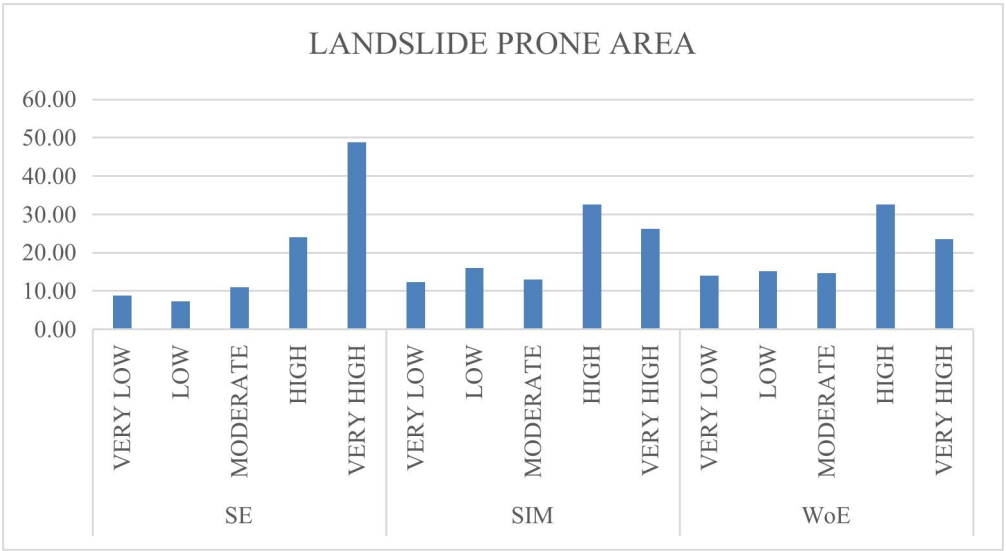

Fig. 6.4 Landslide prone region wise for Darjeeling and Kalimpong

6.3 Result Validation:

In this study, the maps of landslip susceptibility produced by the pertinent models, Shannon Entropy, Statistical Index Method, and Weight of Evidence, were corroborated using the area under the receiver operating characteristic curve technique. The ROC curve was created using the "ROC Tool" in GIS using the landslip data points from the training which were 80% points and testing which were 20% points datasets. The total selected points were 300 out of which 240 were selected as training dataset and 60 for testing dataset, as mentioned earlier.

6.3.1 Area Under the Curve (AUC) of Receiver Operator Characteristics (ROC) Curve:

The Area Under the Curve (AUC) of the Receiver Operator Characteristics (ROC) curve was produced in order to evaluate the effectiveness and accuracy of the landslip susceptibility models. At different threshold settings, the ROC curve compares the true positive rate (sensitivity) with false positive rate (1-specificity). The AUC offers a measurement of the model's overall predictive capacity, with values nearer 1 indicating improved performance.

Three statistical techniques—Shannon's Entropy (SE), Statistical Index Method (SIM), and Weight of Evidence (WoE)—were used in the investigation. Each method's AUC values were examined in order to assess how well each one predicted landslip vulnerability. The SE model produced an AUC value of 0.77, demonstrating its capacity to distinguish between locations that are subject to landslides and those that are not. The WoE model and the SI model both acquired AUC values of 82.5 and 82.6, respectively.

These AUC values show how the SE, SI, and WoE models accurately and consistently predict the vulnerability to landslides. The models' capacity to successfully differentiate between landslide and non-landslide locations based on the chosen conditioning variables is demonstrated by the high AUC values. The findings support the viability of these techniques for mapping landslip susceptibility in the study region, offering useful information for disaster preparedness and land use planning.

True Positive Rate (TPR) and False Positive Rate (FPR) are shown on a ROC curve. The mathematical formula for calculating true positive and false-positive rates is shown in equations 6.1 and 6.2.

$$\text{True Positive Rate} = \frac{TP}{(TP + FN)} \quad (6.1)$$

$$\text{False Positive Rate} = \frac{TN}{(TN + FP)} \quad (6.2)$$

Where,

TP & TN = pixels correctly classified as landslide and non-landslide

FP & FN = pixels incorrectly classified as landslide and non-landslide

The training dataset was used to create the success rate curve (SRC), and the testing dataset was used to create the prediction rate curve (PRC), both utilising the ROC tool.

Below are the various success rate and prediction rate curves for the four used models.

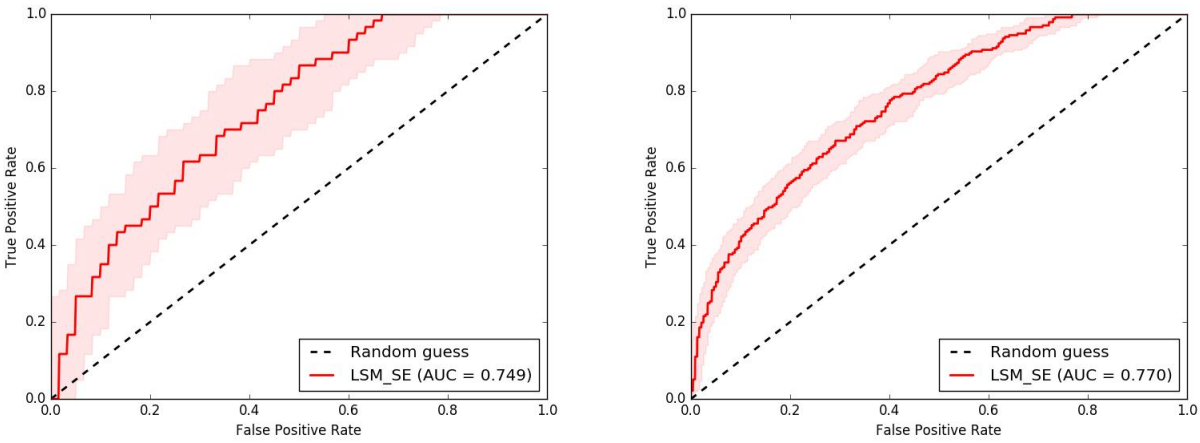

Fig. 6.5 Prediction and Success rate curves for the SE Model

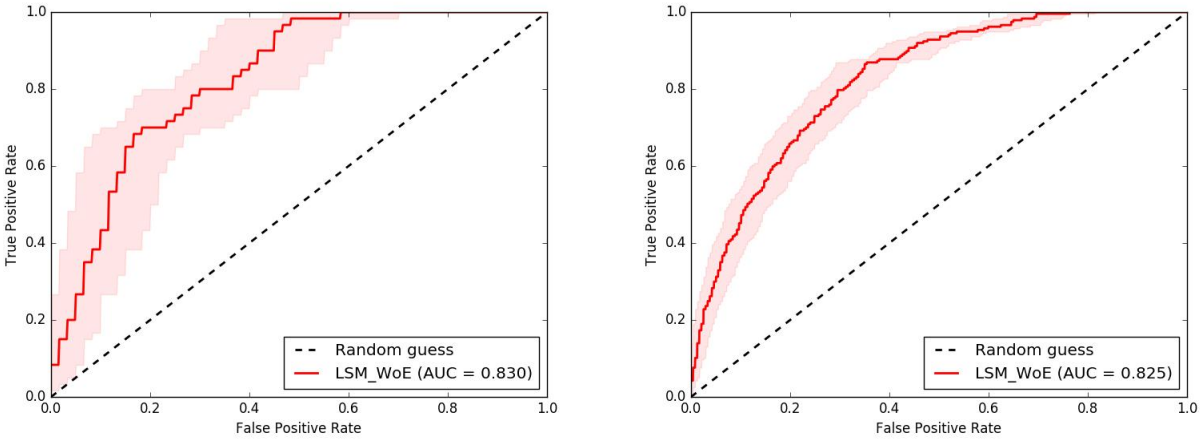

Fig. 6.6 Prediction and Success rate curves for the WoE model

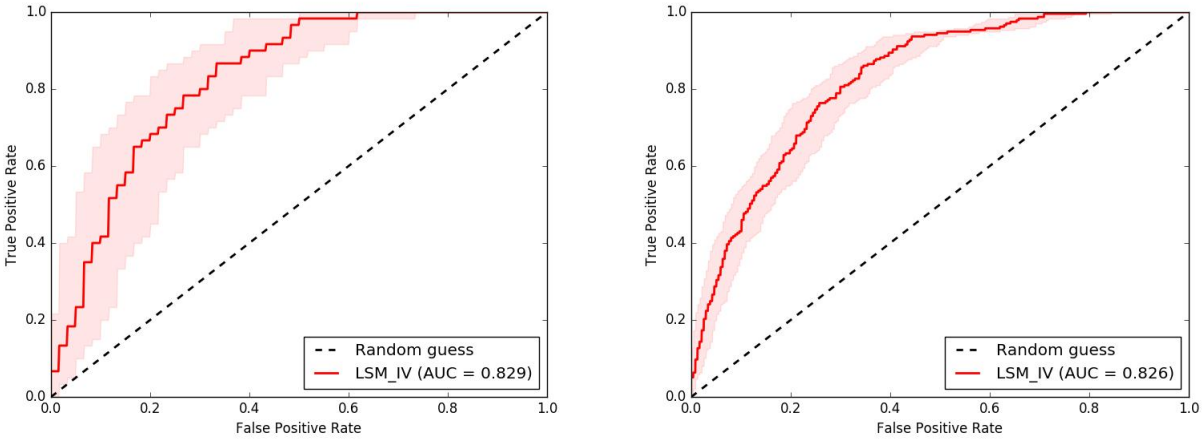

Fig. 6.7 Prediction and Success rate curves for the SI Model

The AUC values for the landslide susceptibility map produced by the Weight of Evidence and Statistical Index Method model are higher than the AUC values for the landslide susceptibility map produced by the Shannon entropy model, as can be seen from success rate curves and prediction rate curves.

Table 6.2 Summary of ROC results for the Models

MODEL	SUCCESS RATE	PREDICTION RATE
SHANON ENTROPY	0.77	0.749
STATISTICAL INDEX	0.825	0.83
WEIGHT OF EVIDENCE	0.826	0.829

CHAPTER 7- CONCLUSION, LIMITATION AND RECOMMENDATION

7.1 Conclusion:

The current study used the Statistical Index Method (SIM), Shannon Entropy (SE), and Weight-of-Evidence (WoE) approaches within a GIS framework to estimate landslip vulnerability in the Darjeeling Kalimpong region of West Bengal, India. The models were developed to predict the likelihood of landslip occurrence by incorporating 13 conditioning factors, including elevation, slope, aspect, curvature, distance to rivers, distance to roads, distance to lineaments, lithology, land use/land cover, stream power index, topographic wetness index, rainfall, and geology.

The results of the SIM model showed that 59% of the study region had high to extremely high landslip susceptibility, while 13% had moderate susceptibility. The SE model identified 73% of the region as highly to extremely sensitive, while 11% was identified as moderately susceptible. In a similar vein, the WoE model classified 15% of the study region as moderately susceptible and 56% of it as extremely to very highly susceptible.

These results emphasise that for mapping landslip risk, a variety of components must be combined with cutting-edge GIS-based approaches. In the research region, the generated models offer crucial insights for planning land use, building infrastructure, and managing disasters. It should be noted that the accuracy of the models was evaluated using the Receiver Operator Characteristics (ROC) curve's Area Under the Curve (AUC). With scores of 0.826 for SIM, 0.77 for SE, and 0.825 for WoE, the findings were favourable.

Overall, this study advances our knowledge of the Darjeeling Kalimpong district's landslip susceptibility and lays the groundwork for further investigation and real-world applications aimed at reducing landslip hazards in the area.

7.2 Limitations:

Despite the interesting results reached from this study on landslip susceptibility mapping using the Statistical Index Method (SIM), Shannon Entropy (SE), and Weight-of-Evidence (WoE) techniques, it's important to acknowledge numerous limitations:

Data calibre and accessibility: The accuracy and reliability of the susceptibility models depend on the calibre and availability of the input data. Data may not always be readily available or may be out-of-date, which might cause ambiguities and limitations in the conclusions.

Scale and resolution: The results of the study are affected by the scale and resolution of the data used. Although more exact and thorough, higher resolution data may not always be practicable to collect or readily available.

The models presuppose that there will always be a link between the conditioning factors and the incidence of landslides. The results of the susceptibility mapping, however, are questionable since these connections might be changed by natural processes and changes in land use.

Limitations of the validation: The validation of the models was only based on the Area Under the Curve (AUC) of the Receiver Operator Characteristics (ROC) curve. Despite being a commonly used statistic, AUC does not provide a comprehensive evaluation of model performance, and additional validation techniques may strengthen the results.

Inaccuracies in the weighting criteria: In both the SE and WoE approaches, weights are given to different training components based on individual assessments. The accuracy of the results depends on how well these weightings are chosen, which might introduce errors and potential biases.

Generalisation of findings: The susceptibility maps produced for the Darjeeling Kalimpong district in West Bengal, India, where the study was performed, are unique to that region. When extending these results to regions with different geological and environmental conditions, exercise care.

Understanding these limitations is essential to effectively interpreting and applying the study's findings. Future estimations of landslip susceptibility may be more accurate if these flaws were fixed and the technique was enhanced.

REFERENCES

[1] A. Chawla, S. Pasupuleti, S. Chawla, A. C. S. Rao, K. Sarkar, and R. Dwivedi, "Landslide Susceptibility Zonation Mapping: A Case Study from Darjeeling District, Eastern Himalayas, India," Journal of the Indian Society of Remote Sensing, vol. 47, no. 3, pp. 497–511, Jan. 2019, doi: 10.1007/s12524-018-0916-6.

[2] A. Saha, V. G. K. Villuri, and A. Bhardwaj, "Development and Assessment of GIS-Based Landslide Susceptibility Mapping Models Using ANN, Fuzzy-AHP, and MCDA in Darjeeling Himalayas, West Bengal, India," Land, vol. 11, no. 10, p. 1711, Oct. 2022, doi: 10.3390/land11101711.

[3] A. Sharma, C. Prakash, and V. Manivasagam, "Entropy-Based Hybrid Integration of Random Forest and Support Vector Machine for Landslide Susceptibility Analysis," Geomatics, vol. 1, no. 4, pp. 399–416, Oct. 2021, doi: 10.3390/geomatics1040023.

[4] A. Yalcin, "GIS-based landslide susceptibility mapping using analytical hierarchy process and bivariate statistics in Ardesen (Turkey): Comparisons of results and confirmations," CATENA, vol. 72, no. 1, pp. 1–12, Jan. 2008, doi: 10.1016/j.catena.2007.01.003.

[5] A. Yalcin, S. Reis, A. C. Aydinoglu, and T. Yomralioglu, "A GIS-based comparative study of frequency ratio, analytical hierarchy process, bivariate statistics and logistics regression methods for landslide susceptibility mapping in Trabzon, NE Turkey," CATENA, vol. 85, no. 3, pp. 274–287, Jun. 2011, doi: 10.1016/j.catena.2011.01.014.

[6] B. Pradhan and S. Lee, "Landslide susceptibility assessment and factor effect analysis: backpropagation artificial neural networks and their comparison with frequency ratio and bivariate logistic regression modelling," Environmental Modelling & Software, vol. 25, no. 6, pp. 747–759, Jun. 2010, doi: 10.1016/j.envsoft.2009.10.016.

[7] B. Pradhan, S. Lee, and M. F. Buchroithner, "Remote Sensing and GIS-based Landslide

Susceptibility Analysis and its Cross-validation in Three Test Areas Using a Frequency Ratio Model," Photogrammetrie - Fernerkundung - Geoinformation, vol. 2010, no. 1, pp. 17–32, Feb. 2010, doi: 10.1127/1432-8364/2010/0037.

[8] B. T. Pham et al., "A comparison of Support Vector Machines and Bayesian algorithms for landslide susceptibility modelling," Geocarto International, vol. 34, no. 13, pp. 1385–1407, Sep. 2018, doi: 10.1080/10106049.2018.1489422.

[9] C. Audisio, G. Nigrelli, and G. Lollino, "A GIS tool for historical instability processes data entry: An approach to hazard management in two Italian Alpine river basins," Computers & Geosciences, vol. 35, no. 8, pp. 1735–1747, Aug. 2009, doi: 10.1016/j.cageo.2009.01.012.

[10] C. J. van Westen, E. Castellanos, and S. L. Kuriakose, "Spatial data for landslide susceptibility, hazard, and vulnerability assessment: An overview," Engineering Geology, vol. 102, no. 3–4, pp. 112–131, Dec. 2008, doi: 10.1016/j.enggeo.2008.03.010.

[11] C.-J. F. Chung and A. G. Fabbri, "Validation of Spatial Prediction Models for Landslide Hazard Mapping," Natural Hazards, vol. 30, no. 3, pp. 451–472, Nov. 2003, doi: 10.1023/b:nhaz.0000007172.62651.2b.

[12] D. Pathak, "Knowledge based landslide susceptibility mapping in the Himalayas," Geoenvironmental Disasters, vol. 3, no. 1, May 2016, doi: 10.1186/s40677-016-0042-0.

[13] D. T. Khuc et al., "Comparison analytical hierarchy process (AHP) and frequency ratio (FR) method in assessment of landslide susceptibility. A case study in Van Yen district, Yen Bai province," Journal of Mining and Earth Sciences, vol. 64, no. 2, pp. 79–90, Feb. 2023, doi: 10.46326/jmes.2023.64(2).08.

[14] F. Guzzetti, A. C. Mondini, M. Cardinali, F. Fiorucci, M. Santangelo, and K.-T. Chang, "Landslide inventory maps: New tools for an old problem," Earth-Science Reviews, vol. 112, no. 1–2, pp. 42–66, Apr. 2012, doi: 10.1016/j.earscirev.2012.02.001.

[15] G. Das and K. Lepcha, "Application of logistic regression (LR) and frequency ratio (FR)

models for landslide susceptibility mapping in Relli Khola river basin of Darjeeling Himalaya, India," SN Applied Sciences, vol. 1, no. 11, Oct. 2019, doi: 10.1007/s42452-019-1499-8.

[16] G. Zhang, Y. Cai, Z. Zheng, J. Zhen, Y. Liu, and K. Huang, "Integration of the Statistical Index Method and the Analytic Hierarchy Process technique for the assessment of landslide susceptibility in Huizhou, China," CATENA, vol. 142, pp. 233–244, Jul. 2016, doi: 10.1016/j.catena.2016.03.028.

[17] H. Pourghasemi, B. Pradhan, C. Gokceoglu, and K. D. Moezzi, "A comparative assessment of prediction capabilities of Dempster–Shafer and Weights-of-evidence models in landslide susceptibility mapping using GIS," Geomatics, Natural Hazards and Risk, vol. 4, no. 2, pp. 93–118, Jun. 2013, doi: 10.1080/19475705.2012.662915.

[18] H. R. Pourghasemi, H. R. Moradi, and S. M. Fatemi Aghda, "Landslide susceptibility mapping by binary logistic regression, analytical hierarchy process, and statistical index models and assessment of their performances," Natural Hazards, vol. 69, no. 1, pp. 749–779, May 2013, doi: 10.1007/s11069-013-0728-5.

[19] H. R. Pourghasemi, M. Mohammady, and B. Pradhan, "Landslide susceptibility mapping using index of entropy and conditional probability models in GIS: Safarood Basin, Iran," CATENA, vol. 97, pp. 71–84, Oct. 2012, doi: 10.1016/j.catena.2012.05.005.

[20] I. Das, A. Stein, N. Kerle, and V. K. Dadhwal, "Landslide susceptibility mapping along road corridors in the Indian Himalayas using Bayesian logistic regression models," Geomorphology, vol. 179, pp. 116–125, Dec. 2012, doi: 10.1016/j.geomorph.2012.08.004.

[21] J. Roy and S. Saha, "Landslide susceptibility mapping using knowledge driven statistical models in Darjeeling District, West Bengal, India," Geoenvironmental Disasters, vol. 6, no. 1, Aug. 2019, doi: 10.1186/s40677-019-0126-8.

[22] J. Roy, S. Saha, A. Arabameri, T. Blaschke, and D. T. Bui, "A Novel Ensemble Approach for Landslide Susceptibility Mapping (LSM) in Darjeeling and Kalimpong Districts, West Bengal, India," Remote Sensing, vol. 11, no. 23, p. 2866, Dec. 2019, doi: 10.3390/rs11232866.

[23] L. Ayalew and H. Yamagishi, “The application of GIS-based logistic regression for landslide susceptibility mapping in the Kakuda-Yahiko Mountains, Central Japan,” Geomorphology, vol. 65, no. 1–2, pp. 15–31, Feb. 2005, doi: 10.1016/j.geomorph.2004.06.010.

[24] M. Mohammady, H. R. Pourghasemi, and B. Pradhan, “Landslide susceptibility mapping at Golestan Province, Iran: A comparison between frequency ratio, Dempster–Shafer, and weights-of-evidence models,” Journal of Asian Earth Sciences, vol. 61, pp. 221–236, Nov. 2012, doi: 10.1016/j.jseaes.2012.10.005.

[25] Nohani et al., “Landslide Susceptibility Mapping Using Different GIS-Based Bivariate Models,” Water, vol. 11, no. 7, p. 1402, Jul. 2019, doi: 10.3390/w11071402.

[26] R. Pellicani, I. Argentiero, and G. Spilotro, “GIS-based predictive models for regional-scale landslide susceptibility assessment and risk mapping along road corridors,” Geomatics, Natural Hazards and Risk, vol. 8, no. 2, pp. 1012–1033, Mar. 2017, doi: 10.1080/19475705.2017.1292411.

[27] S. Chakraborty and S. Mukhopadhyay, “Assessing flood risk using analytical hierarchy process (AHP) and geographical information system (GIS): application in Coochbehar district of West Bengal, India,” Natural Hazards, vol. 99, no. 1, pp. 247–274, Aug. 2019, doi: 10.1007/s11069-019-03737-7.

[28] S. Lee and K. Min, “Statistical analysis of landslide susceptibility at Yongin, Korea,” Environmental Geology, vol. 40, no. 9, pp. 1095–1113, Aug. 2001, doi: 10.1007/s002540100310.

[29] S. Mondal and S. Mandal, “Landslide susceptibility mapping of Darjeeling Himalaya, India using index of entropy (IOE) model,” Applied Geomatics, vol. 11, no. 2, pp. 129–146, Nov. 2018, doi: 10.1007/s12518-018-0248-9.
In-Text Citation: [29]

[30] S. Sarkar, A. K. Roy, and T. R. Martha, “Landslide susceptibility assessment using

Information Value Method in parts of the Darjeeling Himalayas," Journal of the Geological Society of India, vol. 82, no. 4, pp. 351–362, Oct. 2013, doi: 10.1007/s12594-013-0162-z.

[31] T. L. Saaty, L. G. Vargas, and R. Whitaker, "ADDRESSING WITH BREVITY CRITICISMS OF THE ANALYTIC HIERARCHY PROCESS," International Journal of the Analytic Hierarchy Process, vol. 1, no. 2, Dec. 2009, doi: 10.13033/ijahp.v1i2.53

PAPER NAME

Chapters-Parth Jain 2k21gte12.pdf

AUTHOR

parth jain

WORD COUNT

16468 Words

CHARACTER COUNT

85216 Characters

PAGE COUNT

74 Pages

FILE SIZE

2.5MB

SUBMISSION DATE

May 24, 2023 1:12 PM GMT+5:30

REPORT DATE

May 24, 2023 1:13 PM GMT+5:30

9% Overall Similarity

The combined total of all matches, including overlapping sources, for each database.

- 4% Internet database
- Crossref database
- 6% Submitted Works database
- 6% Publications database
- Crossref Posted Content database